INVESTIGATIONS OF SOME ENERGY TRANSFER PROCESSES ASSOCIATED WITH ACETYLACETONATE COMPLEXES OF THE LANTHANOID AND GROUPS I AND II METAL IONS

John Duncan Neilson

A Thesis Submitted for the Degree of PhD
at the
University of St Andrews

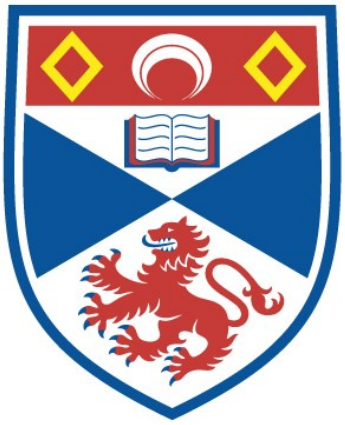

1979

Investigations of some Energy Transfer Processes associated with Acetylacetonate Complexes of the Lanthanoid and Groups I and II Metal Ions

A Thesis

presented for the degree of

DOCTOR OF PHILOSOPHY

in the Faculty of Science of the

University of St. Andrews

by

John Duncan Neilson, B.Sc.

September 1979

University of St. Andrews

Investigations of some Energy Transfer Processes associated with Acetylacetonate Complexes of the Lanthanoid and Groups I and II Metal Ions

J.D. Neilson

Abstract

Intermolecular energy transfer occurs between $Tb(aa)_3.3H_2O$ and $Ln(aa)_3.3H_2O$ complexes (Ln = Pr, Nd, Sm, Eu, Dy, Ho or Er; aa = acetylacetonate) in n-butanol solution at 293K.

Measurement of the decay time of the Tb^{3+} $^5D_4$ level indicates that transfer occurs from this level to excited levels of the Ln^{3+} ions with bimolecular rate constants within the range 0.5 - 4.9 x 10^5 dm^3 mol s^{-1}.

Data from similar measurements on a mixed crystal $Eu_xTb_{(1-x)}(aa)_3.3H_2O$ and other considerations indicate that this is a very short range electron-exchange transfer.

Similar measurements of the Tb^{3+} ion phosphorescence yield indicate the presence of a further intermolecular transfer process between a higher excited state of the Tb^{3+} complex and the added Ln^{3+} complexes. The Stern-Volmer Quenching constants vary from 11 dm^3 mol^{-1} for Ho and Sm to 110 dm^3 mol^{-1} for Pr. It is concluded that this transfer is unlikely to occur from either the ligand singlet or triplet levels and it is proposed that a higher Tb^{3+} level such as the $^5D_3$ may be involved in both inter- and intramolecular energy transfer.

Intermolecular energy transfer between excited state Tb^{3+} ions in $Tb(aa)_3.3H_2O$ and Ln^{3+} ions in $Ln(aa)_3.3H_2O$, where Ln = Eu and Sm, is shown to be markedly solvent dependent. It is proposed that the $Tb^{3+} \rightarrow Ln^{3+}$ energy transfer

occurs in mixed metal dimers where the Tb-Ln distance is likely to be ca. 0.4 nm.

The solvent dependent behaviour is related to the relative concentrations of monomeric and dimeric species in the various solvents. The rate controlling step in the intermolecular energy transfer is probably that of monomer-dimer reaction which at 273K is of the order of 10^5 dm^3 mol^{-1} s^{-1}. The activation energy of this reaction between Tb, Eu and Sm acetylacetonates is estimated to be ca. 23 kJ mol^{-1}.

^1H NMR spectra of $Lu(aa)_3.2H_2O$ in several solvents are reported.

The spectral profiles are temperature dependent in benzene and toluene solutions and the multiplicity of ligand methyl resonances is attributed to slow exchange between non-equivalent methyl groups in a dimeric structure.

The temperature dependence in acetone solution is consistent with the presence of a monomer-dimer equilibrium with ΔH^o = -28.2 ± 1.5 kJ mol^{-1} and $\Delta S^o = -74.5 \pm 4.5$ J K^{-1} mol^{-1}.

The single ligand methyl and 3-H resonances in the strongly coordinating solvents dimethyl sulphoxide and pyridine indicate the sole presence of solvated monomers.

Previous proposals about the anomalous spectrum of $Mg(aa)_2$ in $CDCl_3$ are also discussed.

The extremely low efficiency of the intermolecular enrgy transfer process in europium acetylacetonate compared with the corresponding terbium acetylacetonate is attributed to the presence of a charge-transfer excited state lying below the ligand singlet states. This is supported by the anomalous absorption spectrum of the Eu^{3+} complex and the effects of added anions in other ligand systems.

The phosphorescence spectra of the Group I and Group II metal acetylacetonates (Metal = Li, Na, K, Rb, Cs, Mg, Ca, Sr and Ba) have all been measured in solid Ethanol glass solutions at 77K and found to have profiles similar to that of $Al(aa)_3$.

The phosphorescence decays are non-exponential and this behaviour is attributed to the presence of both coordinated and free acetylacetonate anion.

Time resolved spectroscopy and other considerations indicate that the energies of the lowest excited ligand singlet and triplet states of the aa^- ion are, unlike the triplet state lifetime, little affected by coordination.

Solvolysis is reported in ethanol solution which invalidates some previously reported spectral parameters.

DECLARATION

I declare that this thesis is my own composition, that the work of which it is a record has been carried out by me, and that it has not been submitted in any previous application for a Higher Degree.

This thesis describes results of research carried out at the Department of Chemistry, University of St. Andrews, under the supervision of Dr. T.M. Shepherd since October 1st 1973.

John D. Neilson

CERTIFICATE

I hereby certify that John D. Neilson has spent eleven terms of research work under my supervision, has fulfilled the conditions of Ordinance No. 12 (St. Andrews) and Resolution of the University Court, 1967, No. 1, and is qualified to submit the accompanying thesis in application for the degree of Doctor of Philosophy.

T.M. Shepherd
Director of Research

ACKNOWLEDGEMENTS

I would like to thank Dr. T.M. Shepherd for his help, encouragement and patience during the course of this work.

I am indebted to the Science Research Council for a grant to finance this work, and to Professor Lord Tedder and Professor P.A.H. Wyatt for providing research facilities.

Finally, I wish to thank my wife for her help in typing this thesis.

Summary

Intermolecular energy transfer from $Tb(aa)_3.3H_2O$ to other lanthanoid acetylacetonates has been established. It is proposed that the $^5D_4$ and $^5D_3$ are both donor levels in the Tb^{3+} ion. A comparison between electron exchange and coulombic interaction favours the former, however the rate of intermolecular energy transfer in the crystalline state shows that this is not the rate determining step.

It is further proposed that dimers are formed in some solvents, and that the monomer-dimer interaction is the governing factor in the interspecies energy transfer. The energy transfer from the Tb^{3+} $^5D_4$ level is dependent on solvent. Two reasons are proposed: firstly, the effect on the non-radiative decay routes; and secondly, changes in the rate of interaction of the monomers and dimers.

The absence of Eu^{3+} ion phosphorescence in $Eu(aa)_3.3H_2O$ is attributed to the occurrence of a charge transfer band in this complex.

An investigation of the excited ligand triplet decay in the Groups I and II acetylacetonate complexes in solid ethanol solution shows that the environment of the coordinated acetylacetonate ligand can markedly affect the radiative decay efficiency in a predictable manner.

CONTENTS

Chapter 1

Introduction

1.1. The Rare-Earth Elements[1]

The rare-earth elements form a series of 17 chemically similar metals, all but one of which occur in nature. Often they are called simply rare-earths, but this is a misnomer because the term earth properly should be applied to the oxide. The rare-earth elements are not even particularly rare, though for a long time they were thought to be.

The 17 rare-earth elements are: scandium, yttrium, lanthanum and cerium through to lutetium. The latter group of 14 elements are known as the lanthanoids and the work described in this thesis is largely concerned with these elements.

(a) History of the rare-earths

The Finnish chemist Johann Gadolin in 1794, while investigating a rare Swedish mineral, discovered what he thought was a new element. He named it ytterbia, later renamed yttria. From this same mineral now called gadolinite, another new element was isolated in 1803 and called ceria.

However, it was not until 1808 that Sir Humphrey Davy showed that these earths were not elements but oxides, so that the corresponding elements were given the names yttrium and cerium.

Between 1839 and 1843, Carl Gustaf Mosander in a series of experiments showed that yttria and ceria were mixtures of

oxides. By a long series of fractional crystallisations lanthana and didymia were separated from ceria, and erbia and terbia from yttria. He also managed to isolate the impure metals.

There existed a time of confusion when the existence of these earths was disputed probably due to their considerable similarities in properties. With the introduction in 1859 of the spectroscope, identification of the various earths was much simplified. At about the same time the names of the earths from yttria were interchanged; i.e. erbia became terbia and vice versa.

From 1843 to 1939 further chemical fractionations were undertaken of rare-earth salts isolated from varying minerals. Didymia was resolved into samaria (1879), praseodymia (1885), neodymia (1885) and europia (1901). Terbia and erbia were resolved into holmia (1878), thulia (1879), dysprosia (1886), ytterbia (1876) and lutetia (1907).

Much of the drive in this work was connected with two discoveries of Auer von Welsbach: the Welsbach gas mantle and lighter flint. The gas mantle consisted mainly of 90% thorium nitrate and 10% cerium trinitrate impregnated gauze. When heated with a gas flame the salts were converted to the oxides which when hot gave off an intense white light. The flint compound was a pyrophoric alloy of cerium and iron.

During the search for these compounds it was discovered that the earths were far from being rare. Cerium is more abundant than tin, yttrium and neodymium more abundant than lead and the relatively scarce lutetium more abundant than mercury or iodine. However, although they are relatively abundant on a global scale, they generally occur in most

rock formations at low concentration, typically from ten to a few hundred parts per million by weight.

H. G. J. Moseley while studying x-ray emission spectra discovered the relationship between x-ray frequency and atomic number. By this method the atomic numbers of the rare-earth elements were assigned. It was found that only fourteen lanthanoids could exist and all but one were known. Element 61, promethium, does not occur in nature as no stable isotopes exist, and it was not until 1945 that this element was isolated from the fission products of a nuclear reaction.

(b) Sources of the rare earths

Numerous minerals exist which are rich in the rare-earths, but many are extremely rare or occur as small pockets in more massive rocks. The main commercial minerals are:

1. Monazite; a phosphate of calcium, thorium, cerium and various rare earths, is found in extensive deposits. The lanthanoid content consists mainly of the light elements, i.e. La to Gd.
2. Xenotime; a phosphate of yttrium and various lanthanoids. It contains more of the heavy lanthanoids and is their main source. The mineral is frequently found associated with monazite and can be separated from it magnetically
3. Bastnaesite; a fluorocarbonate mainly of lanthanum and cerium, contains almost exclusively the lighter rare earths and is the source of much of the world's europium.
4. From uranium and apatite mining rare-earths are obtained as by-products although the content of the ores is low.

Niobium titanate minerals e.g. fergusonite, euxenite, samarskite and blomstrandine, as well as the silicates gadolinite and allanite, are rich in the heavy rare-earths, but are not commercially important.

(c) Separation of the lanthanoids

The separation of the lanthanoid elements usually begins with the trivalent ions in dilute solution. The elements which can take on other oxidation states, e.g. Ce(IV), Sm(II), Eu(II) and Yb(II) are removed readily, the remainder are not as easy. Classical techniques of fractionation depended upon dissimilarities in the properties of the ions to be separated, but the trivalent lanthanoids are surrounded by tightly bound water molecules in aqueous solutions and exhibit very similar properties.

However, fractionations are of use in certain cases; for example the method is still used commercially to separate lanthanum and cerium from the heavier lanthanoids. The lanthanium - cerium split is then obtained by making use of the properties of Ce (IV).

Ion exchange is now the most widely applied method of separation of the lanthanoid elements. The method was first applied at the Oak Ridge National Laboratory in 1943 to separate the fission products obtained from nuclear reactors. The method was gradually improved both at ORNL and at Iowa State University where gram quantities of praseodymium and neodymium were first separated.

Ion exchange is a method of separation based on different-

ial absorption and elution of substances from certain solid supporting materials. The ion-exchange elution method is mostly used for analytical work because of the relatively large amounts of solution required for elution and the difficulties in scaling-up. The ion-exchange displacement method is preferred for plant operation.

Liquid - liquid extraction has also been applied to the separation of the lanthanoids, but it is used only in special cases e.g. for Ce and Eu, where as the tetravalent and divalent ions they can be separated relatively easily.

All of these methods make use of the slight variation in the formation constant of a complexing agent with the different lanthanoid ions.

(d) Preparation of the metal lanthanoids

The early methods made use of the metallothermic process whereby one metal replaces another in a compound.

Mosander, in 1826, reduced anhydrous chlorides produced from ceria with metallic sodium and potassium. The yield was low and the resultant metal very impure.

During the next century further attempts were made to produce the metals of the growing numbers of discovered rare-earths. The scope of the metallothermic process was enlarged to encompass the use of magnesium, calcium and aluminium as reductants, and the anhydrous fluorides as the reactants. However, the metals were so impure that no extensive studies could be made of their properties.

Electrolytic processes were partially successful from 1876 onwards, but the recurrent difficulties of cell design to exclude atmospheric impurities and of suitable inert materials for

the containment of the molten rare-earth metal presented extremely difficult problems.

The production of ultra-pure rare-earth metals in recent times has reverted to the metallothermic process. Usually the reductants are calcium or lithium metal and the reactants the anhydrous rare-earth fluorides or chlorides, all carefully purified. The reaction vessels are made of tantalum or tungsten as these have been found to have the least interaction with the rare-earth metals. All apparatus is scrupulously cleaned in ultra high vacuum, and the reactions take place under very high purity inert gas atmospheres. Even with these precautions the resultant metals have small amounts of impurities - principally tantalum or tungsten from the crucibles.

(e) Industrial uses of the lanthanoids

The uses of the rare-earth elements are potentially very wide, but due to their relatively high cost they are replaced whenever possible by less costly materials.

Considerable quantities (about 0.5×10^7 kg in 1969) were used in the U.S. to make catalysts for the cracking of crude oil. On a smaller scale their marked catalytic properties have been used in the hydrogenation of ketones to secondary alcohols, the hydrogenation of alkenes to alkanes, the dehydrogenation of alcohols and butanes, and the formation of polyesters.

The glass industry has substantially replaced rouge by CeO_2 for glass polishing of optical instruments. La_2O_3 as an additive produces high refractive index, low dispersion glasses especially useful in complex lens system. Neodymium

is used to counteract iron impurities which give a yellowish tint, and in its pure form produces purple glass. In conjunction with praseodymium it is employed in welders and glass blowers goggles to absorb the bright yellow light from the sodium flame.

As a scavanger for nonmetallic impurities the rare-earths find extensive use in the metallurgical industry. Removal of impurities from steels and alloys has a range of effects including increasing corrosion resistance, machinability, tensile strength, castability, high temperature workability and decrease in brittleness.

The ultrapure rare-earths find their heaviest use in the television industry where $(Gd, Eu)_2 O_3$ and $(Y, Eu)_2 O_3$ have replaced (Zn, Gd) S as red phosphors. In 1969 the industry consumed greater than 10^4 lbs. of ultrapure $Gd_2 O_3$ and the amount is growing. The rare-earth phosphors have also been incorporated into Hg street lamps where the blue light is converted into intense white radiation similar to daylight. And as the fluorides in the cores of carbon rods, mixed rare-earths are used in searchlights and film projectors.

Y-Fe, Y-Al garnets are employed in the electronics industry. The former can be fabricated in special shapes for use in microwave filters. The latter is also used as imitation diamond because of its high refractive index.

Eu, Gd and Dy have large capture cross sections for thermal neutrons. For this reason they are incorporated in the controlling mechanisms of nuclear reactors. In the control rods they can be used to regulate the reactor or to shut it down completely. They can also be used in a disposable fashion to

even out the reactivity of the reactor with time. As a nuclear reaction proceeds neutron poisons build up at about the same rate as calculated quantities of the rare-earths burn up.

The paramagnetic properties of some rare earth complexes have found widespread use in conjunction with nuclear magnetic resonance spectroscopy to yield information about the configuration of some organic compounds. This procedure has found wide use in the analysis of mixtures of, for example, optical isomers.

(f) Aspects of the handling of the lanthanoids

The lanthanoid salts have low toxicity and can generally be handled without any special precautions. Solutions injected into the peritoneum cause hyperglycemia, hypotension, spleen degeneration and fatty liver. If injected into muscle, 75% remains static, the remainder migrates to the liver and skeleton. Oral ingestion causes only a small proportion to be absorbed by the body. As with other ions, the organically complexed species are more toxic than the solids or inorganic solutions.

The handling of the ores or minerals is complicated however by the co-existence in most of these sources of beryllium, thorium, uranium, etc.

Finally, rare-earth metals when finely divided are pyrophoric, much like magnesium.

1.2. Chemistry of the Lanthanoids

The lanthanoids (Ce-Lu, atomic numbers 58-71) are unique among the elements, except for the closely similar actinoids, in resembling each other so markedly both in the elemental state and in compounds that changes in properties for a given oxidation state with increasing atomic number are largely changes in degree rather than in kind. Typical examples are constancy of a particular thermodynamically stable oxidation state (+3) throughout the series, many instances of isomorphism when both oxidation state and anion are fixed, invariable co-occurrence in nature, the classically striking difficulty in separating one lanthanoid from another, and small differences in the thermodynamic functions for particular reactions of lanthanoid ions of a given charge type. Furthermore, both lanthanum (atomic number 57) and yttrium (atomic number 39), elements treated herein as members of Group IIIA, are broadly indistinguishable from the lanthanoids in so many respects that they are operationally classifiable with the latter. It is, of course, the problems of explanation associated with these situations that prompted early difficulties in the periodic classification of the lanthanoids.

(a) Electronic configurations

Explanation of the aforementioned properties can be found by consideration of the electronic arrangements of the elements and ions.

Scandium, yttrium and lanthanum introduce respectively the first, second and third d-transition series. The configuration of La is therefore the xenon core with three electrons in the

5d and 6s orbitals. Following La, the energy and spatial extension of the 4f orbitals decrease very sharply so that they are within the xenon core and occupied before the remaining 5d orbitals. The filling of these seven well shielded 4f orbitals accounts for the very similar chemical properties of the 14 lanthanoid elements.

(b) Oxidation states

A few solid compounds have been prepared with lanthanoid ions in the +4 state, but only Ce(IV) is sufficiently stable with regard to reduction to be important in aqueous solution.

All the lanthanoid ions have been obtained in the +2 state by entrapment in solid Group II halide matrices, but on dissolution in aqueous conditions, rapid oxidation to the +3 state occurs in all cases bar Eu (II), which oxidises relatively slowly.[2]

Although the +3 state requires in most cases the removal of a 4f electron, once this electron is removed, the remaining electrons in the 4f orbitals are sufficiently shielded by external shells as to be almost unavailable for chemical reaction. In this there is a marked difference to the case of the d-transition ions where the d-orbitals are part of the valency shell.

The overriding stability of the +3 oxidation state in aqueous media has been looked at from the thermodynamic viewpoint by Cunningham.[3] Two conclusions resulted:

(i) Ln^{4+} and Ln^{2+} ions are thermodynamically unstable with respect to the Ln^{3+} ion; Ce(IV) and Eu(II) are on the borderline and are metastable because of slow rates of conversion.

(ii) The stability of the terpositive state is mostly a result of a balance between the ionization and hydration energies of the lanthanoid ions.

(c) Size Relationships

An overall decrease in the size of the atoms and ions is observed with increasing atomic number in the lanthanoid series. This decrease is known as the lanthanoid contraction. As the nuclear charge and the consequent number of 4f electrons increase, the imperfect shielding due to the directional nature of the orbitals allows each 4f electron to experience added electrostatic attraction by the nucleus. This results in a decrease in the size of the $4f^n$ arrangement and therefore of the atoms and ions, with increasing atomic number. Similar effects are observed with the actinoid elements (5f) and to a lesser extent with the d-transition series.

The lanthanoid contraction is responsible for the degree to which some properties of a given oxidation state are expressed. Thus, for the +3 oxidation state, decreasing the crystal radius is associated with:

1. decreasing co-ordination number;
2. decreasing basicity, i.e. increase in degree of hydrolysis, increase in thermodynamic stability, decrease in the decomposition temperature, and alteration of the solubility, etc., for particular types of complex,
3. decrease in ionic character; and
4. decrease in ease of oxidation.

It is these differences in degree that enable separations to be made, be they the classical fractional crystallizations or precipitations, or the more modern ion exchange or solvent extraction techniques.

(d) Bonding

The bonding in Ln^{n+} compounds is generally regarded to be largely ionic.

The binary halides are high-melting, high-boiling crystalline compounds with high conductivities in the molten state, and which dissolve in polar solvents to give conducting solutions. The same is true for the nitrates, perchlorates, bromates, and acetates with due allowance for the thermal stabilities of the anions. Those crystal structures which have been elucidated support the presence of largely ionic bonding in a variety of compound types.

Although the Ln^{n+} ions are relatively large, ions of similar size and oxidation state are known to be ionic; see Table 1.1. Finally, aqueous solution data on the chlorides, bromides, perchlorates, and nitrates of the trivalent lanthanoid ions have given results close to the ideal ratio 1:3[4].

Evidence for minor covalent interactions has been concluded from studies of the thermodynamic and magnetic properties of some chalcogenides, pnictides, borides, and non-stoichiometric halides and oxides[5,6].

(e) Co-ordination

Precise co-ordination numbers can only be unambiguously assigned for crystalline compounds. In aqueous solution the assignment of co-ordination number is difficult, but as an indication of trends, the following hydration numbers of

Ion and radius (nm)		
Lanthanoids	Non-lanthanoids	
Sm^{2+} 0.111	Fe^{2+} 0.083	Pb^{2+} 0.132
Eu^{2+} 0.109	Zn^{2+} 0.083	Ca^{2+} 0.099
Yb^{2+} 0.093	Cd^{2+} 0.103	Sr^{2+} 0.112
La^{3+} 0.106	Al^{3+} 0.051	U^{3+} 0.103
Gd^{3+} 0.094	Cr^{3+} 0.063	Pu^{3+} 0.100
Lu^{3+} 0.085	Rh^{3+} 0.069	Am^{3+} 0.099
Ce^{4+} 0.092	Zr^{4+} 0.079	Th^{4+} 0.099
Tb^{4+} 0.084	Mo^{4+} 0.068	Am^{4+} 0.089

Comparison of lanthanoids with ions of similar charge and size

Table 1.1

the Ln^{3+} ions have been reported: La - Nd, 12.8 ± 0.1; Sm, 13.1; Eu, 13.3; Gd, 13.4; and Dy - Yb, 13.9 ± 0.1[7].

Comparison of the d-transition and the lanthanoid elements brings to light the following points:

1. In the ground state Ln^{n+} ions present prospective ligands with essentially an inert-gas outer electronic arrangement so that the ligand field stabilization energy is relatively small (ca. 4 kJ mol^{-1}).
2. The Ln^{n+} ions are comparatively large.
3. To the Ln^{n+} ions, water is a strong ligand and in general only chelating ligands can displace it to give compounds thermodynamically stable enough to isolate.
4. Ligand exchange reactions are usually very rapid, such that isolable geometric/optical isomers are unlikely.

The lanthanoid ions have therefore more in common with the Group III A cations than with the d-transition ions.

(f) Donor Atoms

Ligands containing oxygen atoms as donors form the most frequently occurring complexes both in solution and the crystalline state. Reaction conditions are important; for example, the formation of rather insoluble hydroxides occur when water is added to Ln Cl_3. xNH_3 and from the addition of strongly basic amines to aqueous Ln^{3+} salt solutions.

The more weakly basic ethylenediamine reacts with perchlorates of the tripositive lanthanoid ions in anhydrous conditions to give $(Ln\ (en)_4)^{3+}$ where the Ln - N bond energy is

ca. 240 kJ mol^{-1}. Nitrogen atoms can act as donors even in the presence of oxygen containing compounds e.g. $Ln(o\text{-phen})_2X_3$, $Ln(o\text{-phen})(C_2H_5OH)X_3$, and $Ln(bipy)_3X_3$, where, o-phen is 1,10-phenanthroline, and X = Cl^-, SCN^-, NO_3^-, $CH_3CO_2^-$.[8] Apart from the halides, most other potential donors, such as P, As, S, and Se, do not form strong bonds.

(g) Thermodynamic stability of complexes in solution

Thermodynamic stabilities of the lanthanoid complexes should refer to their formation from the components under standard state conditions. The free energy change, ΔG°, is then given by:

$\Delta G^\circ = -RT\ln\beta_n = \Delta H^\circ - T\Delta S^\circ$,

where, β_n is the overall formation constant = $K_1K_2K_3....K_n$, (where, K_1, etc. are the stepwise formation constants). Standard conditions are seldom, if ever, used, and indeed concentrations rather than activities are used when discussing equilibrium data.

However, on the basis of β_n values so derived, and ΔH° values gained from calorimetry,[9] it is possible to derive ΔG° and ΔS° terms for the various complexation reactions. It is immediately obvious that lanthanoid ions form less stable complexes than do the d-transition cations of similar charge. This is not unreasonable since ligand-field stabilization is almost totally absent due to shielding of the 4f orbitals, and the charge-to-radius ratio favours the d-transition elements from an electrostatic point of view.

(h) Kinetics of ligand exchange

The kinetics of the lanthanoid reactions are relatively unknown compared to those of the d-transition species. Studies of the kinetics have previously been of two types - relaxation techniques and sampling techniques.

An example of the former is the use of pressure jump[10] in the evaluation of formation and dissociation rates of the 1:1 complex $Ln(C_2O_4)^+$ in aqueous solution. The specific rate constants, k_f, found for oxalate and murexide [11] are shown in Table 1.2. Eigen and Tamm[12] found similar results for other cations and proposed the scheme:

$Ln(aq) + L(aq) \rightleftharpoons Ln(aq)(aq)L \rightleftharpoons Ln(aq)L(aq) \rightleftharpoons LnL(aq) \rightleftharpoons LnL(aq)'$.

The loss of water from the inner hydration sphere (step 3) is slow and therefore rate-determining.

The constancy of k_f for La^{3+} to Eu^{3+} suggests that the inner hydration sphere does not change in this region, but decreases steadily thereafter.

An instance of the second type is the exchange of $^{144}Ce^{3+}$ (radioactive) in polyaminepolycarboxyates of inactive Ce(III)[13]:

$^{144}Ce^{3+} + Ce(L)^{(n-3)-} \rightleftharpoons Ce^{3+} + {}^{144}Ce(L)^{(n-3)-}$

Removal of aliquots followed by counting for the $^{144}Ce^{3+}$ ion yield rate data which are in agreement with initial slow protonation of the complexed ligand followed by extensive rapid protonation and separation of Ce^{3+} ion. Eventually rapid complexation is achieved by radiocerium (III).

	k_f (mole dm^{-3} s^{-1})	
	Oxalate[a]	Murexide[b]
La^{3+}	8.0	8.6
Nd^{3+}	8.6	9.3
Sm^{3+}	8.2	9.6
Eu^{3+}	7.7	8.2
Gd^{3+}	4.6	5.2
Tb^{3+}	2.4	3.0
Dy^{3+}	1.3	1.7
Ho^{3+}	1.0	1.4
Er^{3+}	0.63	1.0
Tm^{3+}	0.63	1.1

a A. J. Graffeo and J. L. Bear, J. Inorg. Nucl. Chem., 30 (1968) 1577.

b G. Geier, Ber. Bunsenges Phys. Chem., 69 (1965) 617.

Formation constants for the species Ln(ligand)

Table 1.2

1.3. Spectroscopy of the lanthanoids

(a) Electronic energy states

The effective shielding of 4f electrons from external fields by the $5s^2 5p^6$ orbitals, causes the electronic energy states that arise from the $4f^n$ configurations to be affected only slightly by the environment, and so to be essentially the same for a given ion in nearly all of its compounds, both in crystals and in solution.[14] As the energy states of the $4f^n$ configurations can be approximated by the Russell - Saunders scheme, and the spin-orbit coupling constants are comparatively large, almost all the +3 ions are characterized by a ground state with a single value of resultant total angular momentum, J, and a first excited state at an energy larger by a number of times the quantity kT. The effect is such that the first excited state is usually only significantly populated at temperatures well above ambient, (Figure 1.1.). Sm^{3+} and Eu^{3+} are exceptions in that they have first excited states whose energy difference from the ground state is less than kT, (300 K), and which are significantly populated in part at room temperature. Indeed, with Eu^{3+}, even the second and third excited states can be populated. The Sm^{3+} and Eu^{3+} ions may be expected to differ from the other Ln^{3+} ions in properties which depend on the relative populations of the J states.

(b) Absorption of radiant energy

Table 1.3 lists the wavelengths of the more important

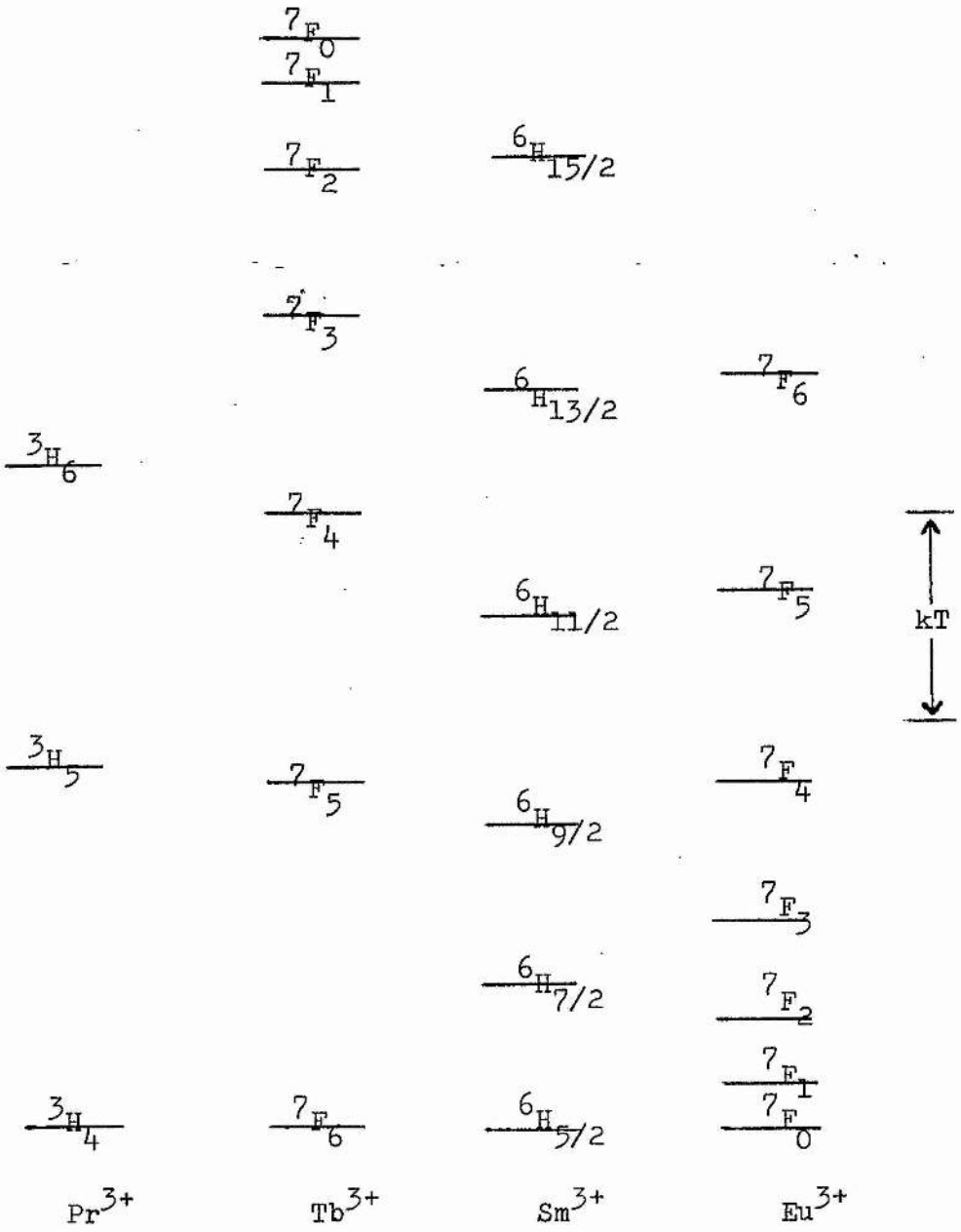

Relative energy levels of ground and excited states for some lanthanoid ions (T = 293 K)

Figure 1.1

Ion	State	Principal absorption bands (nm)	Colour
La^{3+}	$^1S_0$	none	colourless
Ce^{3+}	$^2F_{5/2}$	210.5, 222.0, 238.0, 252.0	colourless
Pr^{3+}	$^3H_4$	444.5, 469.0, 482.2, 588.5	green
Nd^{3+}	$^4I_{9/2}$	354.0, 521.8, 574.5, 739.5, 742.0, 797.5, 803.0, 868.0	reddish
Pm^{3+}	$^5I_4$	548.5, 568.0, 702.5, 735.5	pink
Sm^{3+}	$^6H_{5/2}$	362.5, 374.5, 402.0	yellow
Eu^{3+}	$^7F_0$	375.5, 394.1	colourless
Gd^{3+}	$^8S_{7/2}$	272.9, 273.3, 275.4 275.6	colourless
Tb^{3+}	$^7F_6$	284.4, 350.3, 367.7, 487.2	colourless, pale pink
Dy^{3+}	$^6H_{15/2}$	350.4, 365.0, 910.0	yellow
Ho^{3+}	$^5I_8$	287.0, 361.1, 416.1, 450.8, 537.0, 641.0	yellow
Er^{3+}	$^4I_{15/2}$	364.2, 379.2, 487.0, 522.8, 652.5	reddish
Tm^{3+}	$^3H_6$	360.0, 682.5, 780.0	green
Yb^{3+}	$^2F_{7/2}$	975.0	colourless
Lu^{3+}	$^1S_0$	none	colourless

Wavelengths of important absorption bands of Ln(III) ions

Table 1.3

absorption bands.[15] Although, with the exceptions of Pm^{3+} and Ho^{3+}, ions having the same spectroscopic ground state but differing in the inversion of J values have similar colours, this is coincidental. The bipositive ions are differently coloured from the isoelectronic terpositive species, e.g. red-brown Sm^{2+} vs. colourless Eu^{3+}, straw-yellow Eu^{2+} vs. colourless Gd^{3+}, and green Yb^{2+} vs. colourless Lu^{3+}.

As with the actinoid (5f) ions but in marked contrast to the d-transition species, the lanthanoid ions with the exceptions of Ce^{3+} and Yb^{3+}, have sharply defined bands which are line-like in solution at room temperature. At low temperatures in the crystalline state the spectra resemble those of gases so that the ions can be considered as isolated allowing evaluation of the energy states.

Although strong but structureless bands occur in the UV for the Pm^{3+} - Tm^{3+}, the line-like bands are attributable to the $4f^n$ configurations.[16] The absolute intensities of these bands are small (ε_{max} ca. 0.5) compared with d-transition ions (ε_{max} ca. 10 - 100) and can be explained as due to the shielding of the $4f^n$ configuration by the $5s^2 5p^6$ octet. The transitions are from the ground state $4f^n$ configuration to the same $4f^n$ configuration but with a different J value. The Laporte selection rule forbids an electric dipole transition for a free ion, but the shielding is not complete and the slight distortion caused by the external crystal field causes a small splitting of the states by ca. 100 cm^{-1}.

The $4f^1$ and $4f^{13}$ configurations of Ce^{3+} and Yb^{3+} allow only single values of L so that no internal 4f transitions can occur. The broad bands found are consequences of configurational changes such as $4f^n \longrightarrow 4f^{n-1}5d^1$.

The absorption spectra of the bipositive lanthanoid ions have been obtained after their entrapment in alkaline earth metal halide crystals. The energy states are expected to be similar to the isoelectronic terpositive ions, but with the difference that the energy differences are smaller due to the lesser nuclear charge. As a result the $4f \rightarrow 5d$ transitions are in the visible range of the spectrum, and the Ln^{2+} ion spectra have both the line-like Laporte forbidden bands and the configurational-change bands. The sharp bands appear as superimpositions at much reduced intensity on the broad intense bands.

Complexation alters the spectra of the Ln^{3+} ions only slightly: (1) slight displacements in the bands usually to lower wavelengths; (2) development of fine structure in certain bands; and, (3) changes in intensities of certain bands. The displacements, first noted by Ephraim et al[17], are a function of the anion present and increase with the complexing strength. This nephelauxetic effect[18] is due to inter-electronic repulsion and may be attributed to some degree of covalent interaction.

The development of fine structure and the change in intensities of certain bands are functions of the crystal field strength and symmetry around the lanthanoid ion. The order of perturbation for a lanthanoid ion is:
crystal field < spin-orbit coupling < inter-electronic repulsions.

The limitation of these effects to the "hypersensitive" bands is consistent with the selection rules for quadrupole radiative transitions involving the 4f shell.[19]

(c) Emission of radiant energy

Under UV excitation the anhydrous chlorides of the Ln^{3+} ions in the centre of the series fluoresce strongly. Even in solution Eu(III) compounds fluoresce strongly, and those of Pr(III) and Nd(III) less so. The fluorescent spectra are similar to the absorption spectra, and hence are derived from the 4f configurations.

Weissman[20] reported that excitation of the ligand in some lanthanoid complexes can give rise to fluorescence from the bound lanthanoid ion, a feature which has been exploited in some laser systems.[21]

Whan and Crosby[22] have derived a description of the ligand-cation system which is depicted schematically in Figure 1.2.

Energy is absorbed by the ground-state singlet (S_o) giving rise to an excited-state singlet (S_1). Energy may be lost: (a) non-radiatively to S_o; (b) radiatively to S_o; and, (c) non-radiatively to an excited-state triplet (T_n). Energy so transferred is normally lost by non-radiative transitions to the lowest triplet state (T_1), from whence it may be lost in a manner comparable with the excited-state singlet (S_1). The (c) stage in this case results in an excited-state of the cation. The latter then loses the energy either non-radiatively or radiatively to return to the ground state. The system can therefore give rise to three types of emission: ligand fluorescence, phosphorescence, and metal ion luminescence.

From this scheme a classification of the Ln^{3+} ions has been made:

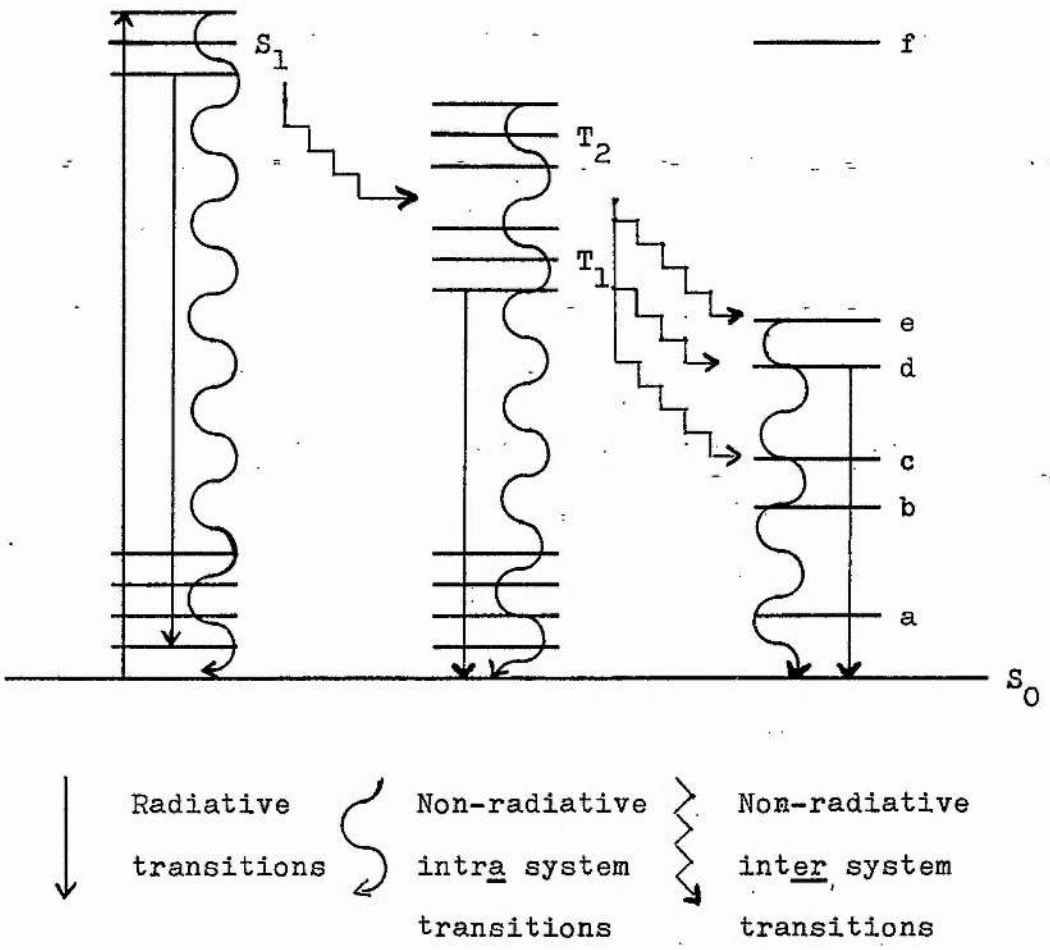

Ligand - cation energy transfer scheme

Figure 1.2

1. No ionic fluorescence. Intra-4f transitions are impossible with La^{3+} ($4f^0$) and Lu^{3+} ($4f^{14}$), and the lowest-lying excited Gd^{3+} ($4f^7$) term is higher than the triplet state energy of most organic ligands.

2. Strong ionic fluorescence. For Sm^{3+}, Eu^{3+}, Tb^{3+}, and Dy^{3+} an excited state of the cation lies closely below the ligand triplet state and there is a relatively large separation between terms.

3. Weak ionic fluorescence. For Pr^{3+}, Nd^{3+}, Ho^{3+}, Er^{3+}, Tm^{3+}, and Yb^{3+} although there is an excited state for each cation lying below the ligand triplet state, the separartions are unsuitable. Furthermore, there are small differences between terms increasing the probability of non-radiative transitions.

A number of the bivalent ions exhibit ionic fluorescence with Sm^{2+}, Dy^{2+}, and Tm^{2+} having lasing properties.[23]

References

Chapter 1.

1. Encyclopaedia Britannica. 15th edition.

2. L.B. Asprey et al., Prog. in Inorg. Chem., vol. II, pp. 267-302. Interscience Publishers, N.Y., 1960.

3. B.B. Cunningham, XVIIth Internat. Cong. of Pure and Appl. Chem., Munich, 1959, pp 64-81, Butterworths, London, 1960.

4. F.H. Spedding et al., J. Amer. Chem. Soc., 74 (1952) 2055, 2778, 2781, and 4751;
ibid., 76 (1954) 879, 884;
J.L. Dye et al., J. Amer. Chem. Soc., 76 (1954) 888.

5. E.F. Westrum, Jr, Prog. in the Sc. and Technol. of the R.Es. (L. Eyring, ed.), vol.1 (1964), pp 310-350, vol.2 (1966), pp 35-89, vol.3 (1968), pp 459-514, Pergamon Press, N.Y.

6. G. Brauer, ibid., vol.1 (1964), pp 152-166, vol.2 (1966), pp 312-339, vol.3 (1968), pp 434-458;
J.D. Corbett et al., Lanthanide/Actinide Chemistry, vol.71, pp 56-66, Advances in Chem. Ser., A.C.S., Washington, 1967.

7. G.R. Choppin et al., Inorg. Chem., 4 (1965) 1254.

8. F.A. Hart et al., J. Inorg. Nucl. Chem., 26 (1964) 579, 27 (1965) 1605, 1825; Proc. Chem. Soc., (1963) 107.

9. I. Grenthe, Acta Chem. Scand., 17 (1963) 2487, 18 (1964) 283, 293;
I. Grenthe et al., ibid, 17 (1963) 2101;
J.L. MacKey et al., J. Amer. Chem. Soc., 84 (1962) 2047;
P.L.E. de la Praudiere et al., J. Inog. Nucl. Chem. 26 (1964) 1713;
L.A.K. Staveley et al., Nature, 211 (1966) 1172; J. Inorg. Nucl. Chem. 30 (1968) 231.

10. A.J. Graffeo et al., J Inorg. Chem. 30 (1968) 1577.

11. G. Geier, Ber. Bunsenges. Phys. Chem., 69 (1965) 617.

12. M. Eigen et al., Z. Elektrochem., 66 (1962) 93, 107.

13. P. Glentworth et al., J Inorg. Nucl. Chem., 30 (1968) 967.

14. B.G. Wybourne, Spec. Prop. of the Rare Earths, Interscience Publishers, N.Y., 1965.

15. W Prandtl et al., Z. anorg. u. allgem. Chem., 220 (1934) 107;
T. Moeller et al., Anal. Chem., 22 (1950) 433;
T. Moeller et al., J. Amer. Chem. Soc., 73 (1951) 3149;
C.V. Banks et al., Anal. Chim. Acta, 15 (1956) 356;
D.C. Stewart et al., Anal. Chem., 30 (1958) 164;
W.F. Meggars et al., J. Res. Nat. Bur. Stds., 46 (1951) 85;
J.B. Gruber et al., J. Inorg. Nucl. Chem., 14 (1960) 303.

16. D.M. Yost et al., The Rare Earth Elements and their Compounds ch.3, John Wiley, N.Y., 1947.

17. F. Ephraim et al., Ber. Bunsenges. Phys. Chem., 59 (1926) 2692, 61 (1928) 65, 72, 62 (1929) 1509,1520, 1639;
F. Ephraim, ibid., 61 (1928) 80.

18. C.E. Schäffer et al., J. Inorg. Nucl. Chem., 8 (1958) 143;
C. Klixbüll Jørgensen, Prog. in Inorg. Chem., vol.4 pp 73-124, (F.A. Cotton, ed.), Interscience Publishers, N.Y., 1962;
C. Klixbüll Jørgensen et al., Z. Naturforsch., 19(a) (1964) 424.

19. C. Klixbüll Jørgensen et al., Mol. Physics, 8 (1964) 281.

20. S. I. Weissman, J. Chem. Phys., 10 (1942) 214.

21. A. Lempicki et al., Phys. Letters, 4 (1963) 133;
T. Moeller et al., Prog. in Sc. and Technol. of the Rare Earths, vol.3 pp 61-128, (L. Eyring, ed.), Pergamon Press, N.Y., 1968;
S.P. Sinha, Complexes of the Rare Earths, Pergamon Press, N.Y., 1966.

22. R.E. Whan et al., J. Mol. Spect., 8 (1962) 315.

23. P.N. Yocom, Proc. 6th Rare Earth Res. Conf., pp.228-238, (Gatlinburg, Tenn., May 3-5, 1967), Oak Ridge National Laboratory, Oak Ridge, Tenn.

Chapter 2

Experimental Methods

2.1. Preparation of hydrated lanthanoid acetylacetonates

The oxides of the lanthanoid (III) ions were refluxed in 50 % hydrochloric acid solutions until dissolution. Excess hydrochloric acid was removed under low pressure on a rotary evaporator with successive additions of distilled water. Care was exercised to ensure that no hydrolysis occurred to the oxyhalides which are insoluble in water.

Ammonium acetylacetonate solution was prepared by the addition of 1 mole equivalent of "0.88 ammonia" solution to a suspension of acetylacetone in a small amount of water.

The lanthanoid (III) chlorides were dissolved in a minimum of water, and to these solutions was added dropwise a solution of 3.5 mole equivalents of ammonium acetylacetonate. By adjusting the pH of the solution (if necessary by the addition of dilute 'ammonia' solution) in the range of pH 6-7, heavy precipitation of product was obtained - the point of maximum yield varying with lanthanoid ion (see Table 2.1). When all the ammonium acetylacetonate had been added, the mixture was allowed to stir for approximately one hour to allow complete reaction to occur:

$$3NH_4aa_{(aq)} + LnCl_{3(aq)} = Ln(aa)_3.nH_2O + 3Cl^-_{(aq)} + 3NH^+_{4(aq)}$$

N.B. It was necessary to ensure that the pH did not rise much above the maximum yield point to minimise hydrolysis.

pH	Lanthanoid
6.9	Cerium
6.6	Praseodymium, Neodymium
6.5	Samarium, Europium, Gadolinium
6.4	Terbium, Dysprosium, Holmium
6.3	Erbium
6.1	Ytterbium

pH of solution at which the maximum yield of tris-acetylacetonate complex is obtained

Table 2.1

The precipitate was filtered off under vacuum, washed with a minimum of water, and dried briefly over calcium chloride. The product was purified by dissolving in the minimum of ethanol with heating, addition of a few drops of acetylacetone to retard hydrolysis, and the addition dropwise of sufficient distilled water to produce a 60 % ethanol solution. The solution was then allowed to cool, and the crystallised product filtered off under vacuum, washed with a minimum of 50 % ethanol solution, and dried briefly over calcium chloride. The tris-acetylacetonate complexes were stored in stoppered vials to prevent the loss of water of crystallization. Analysis of the compounds was performed using a Perkin Elmer Model 240 elemental analyser. The results obtained are given in Table 2.2.

2.2. Preparation of Groups I and II acetylacetonate complexes

The methods used were developed from the general method of Job and Goissedet[1].

The Group I complexes were prepared by adding dropwise a solution of the metal hydroxide in the minimum volume of water to a stirred ethanolic solution of redistilled acetylacetone (1-2 mol equivalents). The complexes were precipitated immediately in all cases except Rb and Cs where they separated on standing.

The Group II complexes were prepared by adding a near saturated ethanol solution of ammonium acetylacetonate (2.4 mole equivalents) to a stirred aqueous solution of the metal chloride. The complexes separated immediately or after standing

Compound	Formula mass	$\%C_{calc.}$	$\%H_{calc.}$	$\%C_{found}$	$\%H_{found}$
$La(aa)_3.3H_2O$	490.3	36.75	5.55	36.81	5.56
Ce "	491.5	36.66	5.54	36.59	5.54
Pr "	492.3	36.60	5.53	36.66	5.57
Nd "	495.6	36.35	5.49	36.38	5.66
Sm "	501.8	35.91	5.42	35.89	5.42
Eu "	503.3	35.80	5.41	35.67	5.36
Gd "	508.6	35.42	5.35	35.26	5.28
Tb "	510.3	35.31	5.33	35.28	5.43
Dy "	513.9	35.06	5.30	35.03	5.04
Ho "	516.3	34.90	5.27	35.16	5.33
Er "	518.6	34.74	5.25	34.72	5.20
Tm "	520.3	34.63	5.23	34.60	5.21
Yb "	524.4	34.36	5.19	34.10	5.17
$Lu(aa)_3.2H_2O$	508.3	35.44	4.96	35.71	4.97

aa is the pentan-2,4-dionato anion, $(C_5H_7O_2)^-$

Carbon and hydrogen analyses of the lanthanoid chelates

Table 2.2

for 1 to 2 hours. The crude Group I and Group II complexes were washed with a minimum volume of water and dried in vacuo. They were recrystallised from 95% ethanol containing some acetylacetone, and finally dried in vacuo at room temperature for 12 hr.

These methods produced anhydrous complexes (M= Li and Mg), partially hydrated complexes (M= Na, K, Ca, Sr and Ba), and materials for which the analytical results (Table 2.3) indicated the prescence of some metal hydroxide (M= Rb and Cs). The hygroscopic nature of these complexes indicates that the anhydrous complexes can only be prepared under rigorously anhydrous conditions. Since the experimental measurements to be described were carried out in 95% ethanol, complete dehydration of the complexes was not attempted.

$Al(aa)_3$ was prepared by a literature method[2].

2.3. Purification of solvents[3]

(a) n-Butanol

Solvent n-butanol was dried by treatment with sodium metal, followed by reflux with an appropriate amount of di-n-butylphthalate, before fractional distillation.

(b) Benzene

Solvent benzene was distilled over sodium metal wire, and redistilled before use.

(c) Acetonitrile

Solvent acetonitrile was treated with calcium hydride until no further hydrogen was evolved. After fractional distillation over P_2O_5, the solvent was finally distilled from anhydrous K_2CO_3.

Compound	Formula mass	%$C_{calc.}$	%$H_{calc.}$	%C_{found}	%H_{found}
Li(aa)	106.0	56.63	6.65	56.22	6.55
$Na(aa).1.6H_2O$	150.9	39.79	6.81	39.91	6.74
$K(aa).0.9H_2O$	154.4	38.89	5.74	38.62	5.43
$Rb(aa)_{0.7}(OH)_{0.3}$	159.9	26.28	3.28	26.66	3.52
$Cs(aa)_{0.8}(OH)_{0.2}$	215.6	22.28	2.71	22.61	2.68
$Mg(aa)_2$	222.5	53.97	6.34	53.64	6.19
$Ca(aa)_2.0.5H_2O$	247.3	48.57	6.11	49.02	6.45
$Sr(aa)_2.1.5H_2O$	312.9	38.39	5.48	38.36	5.62
$Ba(aa)_2.0.7H_2O$	248.2	34.80	4.50	34.52	4.29
$Al(aa)_3$	324.3	55.57	6.53	55.45	6.80

aa is the pentan-2,4-dionato anion, $(C_5H_7O_2)^-$

Carbon and hydrogen analyses of the Group I, Group II, and Al complexes

Table 2.3

(d) Acetone

Solvent acetone was treated at reflux with small portions of $KMnO_4$ until the violet colour persisted, followed by distillation from anhydrous K_2CO_3.

(e) Benzonitrile

Solvent benzonitrile was dried over anhydrous K_2CO_3, and distilled from P_2O_5 in an all-glass apparatus under reduced pressure, collecting the middle portion.

(f) Ethylene Glycol

Solvent ethylene glycol was dried with anhydrous $MgSO_4$, and distilled under vacuum. The distillate was treated with sodium metal under nitrogen, refluxed for several hours, then distilled under vacuum.

(g) Pyridine

Solvent pyridine was refluxed over solid KOH, followed by fractional distillation.

(h) Dimethyl Sulphoxide

Solvent dimethyl sulphoxide was dried over anhydrous $CaSO_4$, followed by fractional distillation under reduced pressure.

(i) Carbon Tetrachloride

Solvent carbon tetrachloride was washed with distilled water, dried over anhydrous K_2CO_3, followed by fractional distillation.

2.4. Ground state absorption spectroscopy

Absorption spectra of all compounds were obtained using the appropriate solvent as reference unless otherwise stated.

In the ultraviolet and visible regions, the measurements

were obtained using a Perkin-Elmer Model 402 spectrophotometer. This has a double beam optical null system, and covers the range 190 to 850 nm by means of air-cooled deuterium lamp for 190 to 390 nm, and a ribbon-filament tungsten lamp for the visible region. All the measurements were carried out in optically balanced fluorescence quartz cells with PTFE stoppers. All optical densities were recorded at ambient temperature, and the extinction coefficients are quoted in units of $cm^{-1}mol^{-1}l$, unless otherwise stated. The units of extinction coefficient may be converted to SI units, m^2mol^{-1}, by multiplying by 10.

2.5. Emission spectroscopy

Two spectrofluorimeters were used to obtain emission spectra, both in the solid and solution states, and these are described below in paragraphs (a) and (b).

(a) Perkin-Elmer Hitachi MPF-2A

The MPF-2A, in conjunction with its phosphorescence, solid sampler, and constant temperature cell holder accessories, allowed measurement of emission and excitation spectra of solids and solutions over the temperature range 77K to ambient.

The MPF-2A uses a standard R106 photomultiplier and two 600 lines per mm grating monochromators. The excitation range is 200 to 700 nm, while the emission range is 200 to 800 nm. Both monochromators are continuous within their respective ranges. Resolution of the spectra is dependent on the excitation and

emission slit widths, which can be set to give band passes of between 1 and 40 nm.

Excitation spectra were obtained by setting the emission monochromator at or near the wavelength of maximum emission, and scanning with the excitation monochromator. In a similar fashion, the emission spectra were obtained by exciting the sample at or near its absorption maximum, by a suitable setting of the excitation monochromator, and scanning with the emission monochromator.

The light source is a 150 W Xenon lamp, giving a near-continuum from ca. 270 to 800 nm. Changes in source -light intensities during scanning procedures, could be directly compensated for by using the instrument's "reference" mode. Before dispersion at the excitation monochromator, the light beam is split; one portion being focussed onto a photomultiplier where a signal is produced which is used as a reference. The other portion is passed through the sample in the normal way. The resultant "sample" signal produced by the R106 photomultiplier is then biased by the reference signal before passing on to the recording device.

It was found that experimental investigations lasting for relatively short times could be undertaken on the "direct" mode, as only minor fluctuations in the lamp intensity occurred.

(b) <u>High resolution spectrofluorimeter</u>

A locally designed spectrofluorimeter was used to measure high resolution spectra of samples over a temperature range

of 77K to ca. 360K. It consists of a 1200 lines per mm emission monochromator incorporated in a Hilger-Watts Monospek 1000. The light source is a water cooled medium pressure mercury lamp, filtered to pass only the 365.5 nm radiation. The exciting light is focussed onto the sample which can be set at any angle to the incident radiation by means of a rotatable cell; the latter being located in a four-windowed dewar; (see Figure 2.1). Light emitted from the sample is focussed onto the incident slits of the monochromator; the dispersed light from the monochromator's excident slits is focussed onto the EMI 9526 photomultiplier. The signal to noise was enhanced by using a phase-sensitive detector, (Brookdeal Electronics), before subsequent amplification and transfer to the recording device.

The solution and solid sample cells used in conjunction with the Monospek are illustrated in Figures 2.2 and 2.3, respectively, and the high resolution system, in Figure 2.4.

(c) Sampling techniques

The great effect that impurities can produce in spectroscopic measurements has been emphasized by many authors; consequently, great care was taken in the preparation of materials. Glassware was immersed in chromic acid, thoroughly washed with distilled water, and well dried before use. Solvents and organic reagents were all purified before use as previously detailed. All prepared chelates under investigation were submitted for analysis.

Emission spectral profiles were recorded using the right-angled viewing technique. Molecules having overlaps between

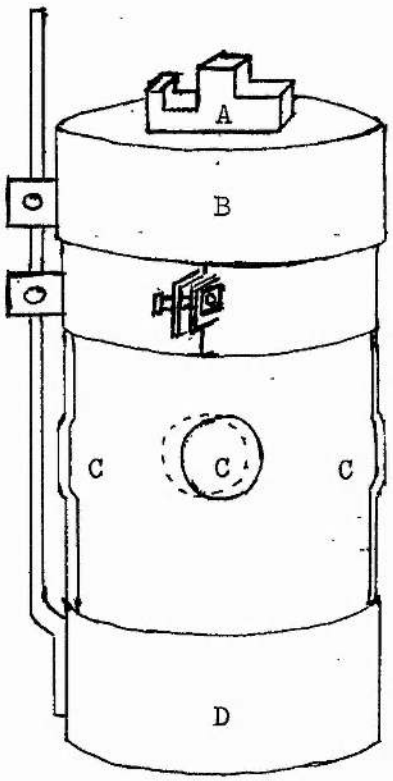

A. Cell housing. B. Polystyrene insulated lid.

C. Quartz windows. D. Stand.

Sample dewar

Figure 2.1

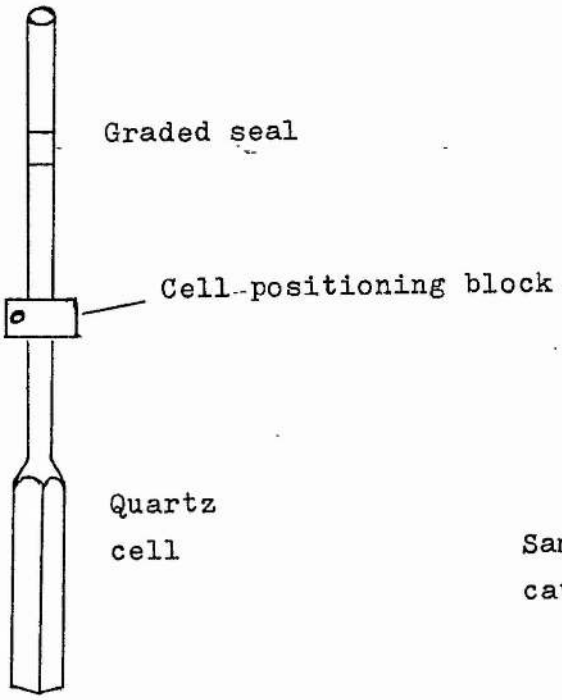

Solution cell

Figure 2.2

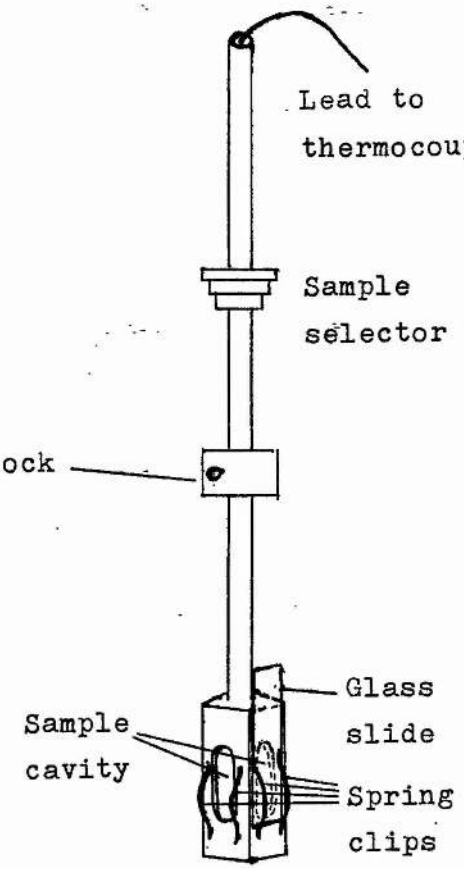

Solid sampler

Figure 2.3

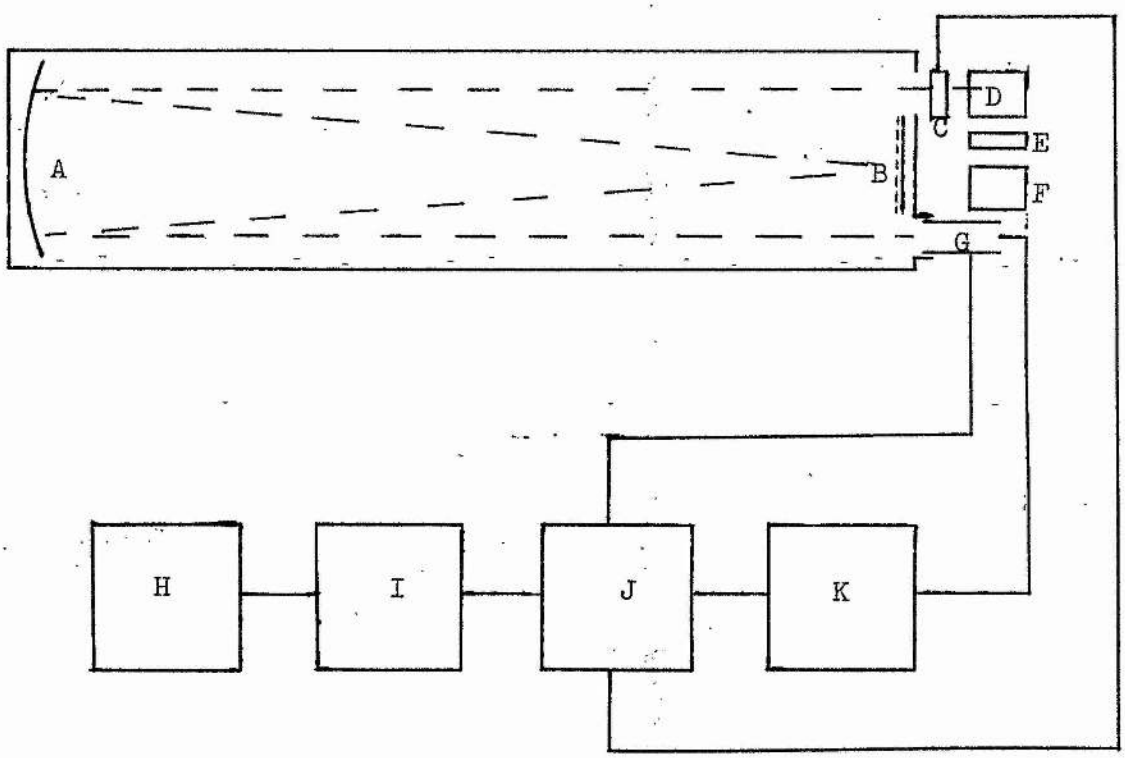

A. Mirror. B. Monochromator. C. Chopper. D. Sample holder. E. Filter. F. Mercury lamp. G. Photomultiplier. H. Recorder. I. Amplifier. J. Phase sensitive detector. K. Photomultiplier power supply.

Schematic diagram of the high resolution spectrofluorimeter

Figure 2.4

their emission and absorption bands, may exhibit self-absorption of emission, usually known as the inner filter effect. This effect is usually avoided by employing very dilute solution (optical density < 0.02) otherwise corrections have to be made. However, in the case of the lanthanoid chelates, emission is shifted far to the red relative to the absorption bands, and so, no limitations are imposed on concentration from this effect.

Numerous molecules are quenched by dissolved oxygen in fluid or solid solutions, and precautions usually have to be taken to prevent such quenching when measuring quantitative luminescence. Comparison of quantitative measurements using degassed, and untreated solutions have indicated that oxygen quenching is not an important deactivation process with the lanthanoid chelates under investigation, hence no initial degassing procedures were employed in this work.

Front-face illumination was used in the investigations of energy transfer between different lanthanoid chelates in solution, as this is the best method for measuring quantitative emission from concentrated solutions. The cell was held at an angle of ca. 30° to the incident beam, which was defocussed, causing most of the sample to be illuminated. The reproducibility of the measurements thereby was improved by minimising the errors that can arise from slight positional changes of cell between samples.

(d) Correction of emission spectra

An absolute fluorescence spectrum is a plot of fluorescence intensity, measured in relative quanta per unit wavenumber interval, against wavenumber. When a spectrofluorimeter is used

at constant slit width and constant detector sensitivity, the curve obtained is the apparent emission spectrum.[4] To determine the absolute spectrum, the apparent curve has to be corrected for changes in sensitivity of the photomultiplier, the bandwidth of the monochromator, and the transmission of the monochromator with wavenumber. Thus, if $dQ/d\nu$ represents the fluorescent intensity at any wavenumber ν, the observed photomultiplier output, A_ν, which corresponds to the apparent emission spectrum is given by:

$$A_\nu = (dQ/d\nu)P_\nu B_\nu L_\nu = (dQ/d\nu)S_\nu; \qquad \ldots\ldots 2.1$$

where P_ν is the output per quantum from the photomultiplier at wavenumber ν; B_ν is the bandwidth in wavenumber units at wavenumber ν; L_ν is the fraction of light transmitted by the spectrofluorimeter at wavenumber ν.

The quantity S_ν is the spectral sensitivity factor of the monochromator-photomultiplier combination. The absolute emission spectrum is calculated from the apparent emission spectrum by dividing it point by point by S_ν. The spectral sensitivity curve may be obtained in various ways:[5]

i) by a calibrated tungsten lamp (for the visible region);

ii) by a fluorescence screen monitor (for the ultraviolet region);

iii) by a thermopile;

iv) by fluorescent solutions which function as quantum counters;

v) by reference solutions, the absolute fluorescence spectrum of which have been determined previously.

Both spectrofluorimeters were calibrated using method (v). If the absolute luminescent spectrum has been determined precisely for a series of compounds that emit over the range for which a spectral sensitivity factor is required, then the

measurement of the uncorrected spectra of the compounds with the system to be calibrated, permits direct calculation of S_λ by direct application of Equation 2.1.

The compounds and the experimental technique used to obtain the sensitivity factors have been discussed by J. F. Ireland.[6]

Calibration of the MPF-2A was carried out by Ireland,[6] and that of the Monospek by Dean.[7] Comparison of the two sets of values shows the better response characteristics of the EMI 9526 compared to the R 106 photomultiplier, especially in the red region of the spectrum.

(e) Automatic digitalisation and correction of emission spectra

Manual correction of emission spectra can be very time consuming, especially with complicated spectra. Computers, therefore, have been employed in this task,[8,9] but their full potential can only be realised if the spectral data can be conveniently and rapidly assembled in computer-readable form. The apparatus described below achieves this using automatically punched paper tape (see also Figure 2.5).

The output from the spectrofluorimeter is connected to a Solartron LM 1604 digital voltmeter (DVM) with an EX 3054 positive logic fan-out unit. The voltmeter is interlinked with a Solartron 3230 data transfer unit (DTU) and a Facit 4070 paper tape punch. This arrangement enables the detector voltage of the spectrofluorimeter to be sampled and recorded at rates up to a maximum of about four samples per second. Slower sampling rates are obtained by initiating the sample cycle with a variable square-wave generator.

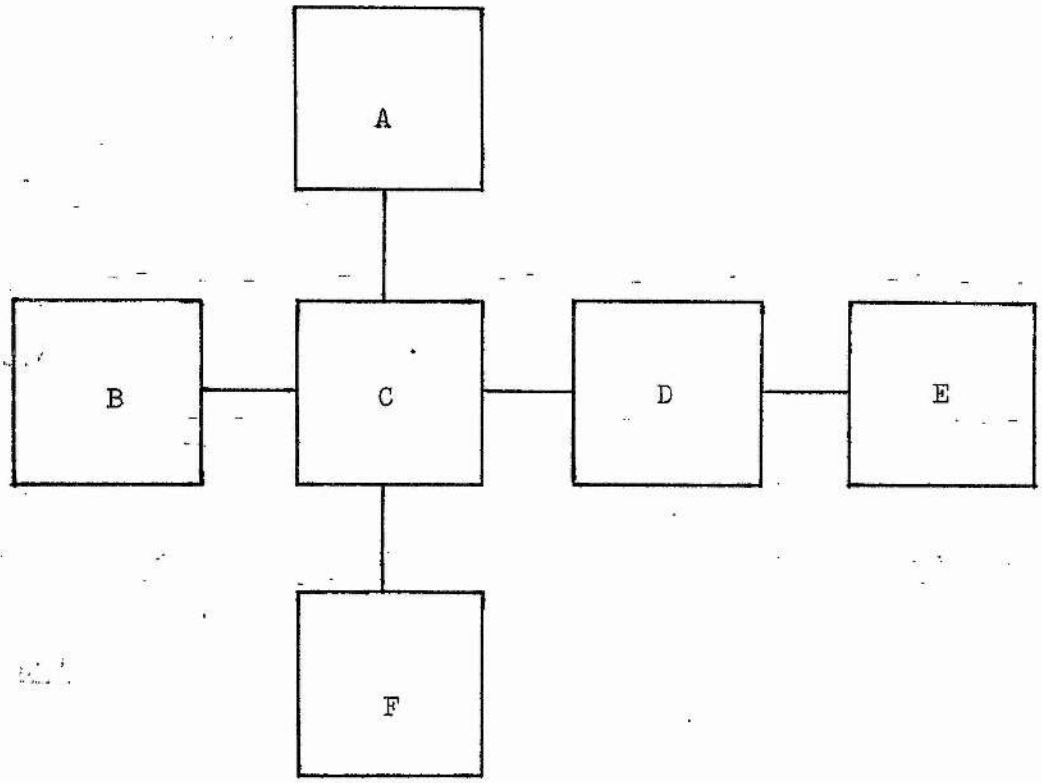

A. Manual entry unit. B. Square-wave generator. C. Digital transfer unit; DTU. D. Digital voltmeter; DVM. E. Spectro-fluorimeter. F. Paper tape punch; PTP.

Schematic diagram of the automatic digitalisation apparatus

Figure 2.5

(f) Operation

To record a spectrum over the wavelength region λ_1 to λ_2, the tape punch is operated only between these limits. A symbol indicating the end of the data set is punched on the tape via a Solartron 3209 manual entry unit. Since the wavelength scan is linear with time the wavelength corresponding to the n^{th} record on the tape may be computed:

$$\lambda_n = \lambda_1 + (n-1)(\lambda_2-\lambda_1)/(N-1); \quad \ldots\ldots 2.2$$

where N is the total number of records.

N is counted during the subsequent processing of the tape, and a spectrum identification code number is manually punched before each spectrum is recorded. The tape is now a digital record of the uncorrected spectrum and can be processed in conjunction with a predetermined response function to give a corrected spectrum.

(g) Computer processing

The computer used was an IBM 360/44 with a Honeywell 3091 paper tape reader. The programming was done in Fortran IV with the exception of a short translation in PL 360. The program SPECTRUM was used, which supersedes SPEKA and SPEKB[6], and a brief description follows.

SPECTRUM incorporates spectral correction factors for both the MPF-2A (emission and excitation) and the Monospek, and will correct spectra for changes in photomultiplier sensitivity and source fluctuations with change in wavelength. It allows corrected spectra, which have been normalised to 100 units intensity, to be plotted as a function of wavelength and wavenumber.

It also allows:

i) averaging of several spectra to reduce noise;

ii) integration of area under the corrected spectrum;

iii) subtraction of blanks to allow for changing baseline;

iv) plotting of inserts to show magnified sections of the spectrum;

v) storing of spectra on magnetic tape whereby a particular spectrum may be replotted in a different format. It provides a line-printer output of wavelength with corresponding normalised corrected intensities, the increment between each wavelength reading and the normalised factor, which is the figure by which the largest corrected intensity value is multiplied to produce a value of 100 units. The various options required are requested on control cards submitted along with the tape before processing. The program SPECTRUM was written by Drs. C. R. S. Dean and T. M. Shepherd.

2.6. Excited state lifetime measurements

Two basic techniques have been generally used for direct measurement of excited state lifetimes.[10,11] The first method, introduced by Gaviola,[12,13] is that of phase and/or modulation fluorimetry. The phase and/or modulation of the fluorescent or phosphorscent emission is compared with the phase and/or modulation of the exciting light. In the second method, pulse fluorimetry, the sample is excited by intermittent light pulses of short duration, and the fluorescence decay is observed directly during the intervals between the excitation pulses. This method requires a light pulse source which cuts off in a time shorter than or comparable with the fluorescence lifetime, and a detector system with a fast response time.

Several modifications of the two basic techniques are described in reviews by Ware[11] and Birks.[14]

(a) Description of apparatus

A schematic representation of the apparatus used to obtain lifetimes of fluorescent solids and solutions over the temperature range 77K to ca. 330K is given in Figure 2.6.

Fluorescence from the particular emission band of interest is detected normal to the exciting light by adapting the Monospek 1000. Two excitation sources were employed:
i), for most of the work, a flash tube of energy rating 10-20 J and ca. 1 ms duration; and,
ii), for the work in Chapter 7, a 125 W high pressure mercury lamp with associated mechanical shutter. The firing of the flash tube and the operation of the shutter were synchronised electronically with the signal averager, (Data Laboratories 200, DL 102, 200 point averager). After a predetermined delay, the photomultiplier output is sampled for a period of time and the curve stored. The sample cycle may be repeated for 2^n sweeps (where n = 1 to 8) and the curves averaged to give an enhanced signal to noise ratio. The averaging procedure and the final decay curve are monitored on an oscilloscope. The stored curve is transferred onto paper tape by means of the data transfer unit previously described. Subsequent processing of the tape was carried out by computer. For simple exponential decreases, the program LIFETIME was used. In the case of the results in Chapter 7, an iterative program was used to solve the relationship:

$$X_{(t)} = A \exp(-t/Y) + B \exp(-t/Z) \quad \ldots\ldots 2.3$$

The program has the limiting condition that if $Z \gg Y$, then as

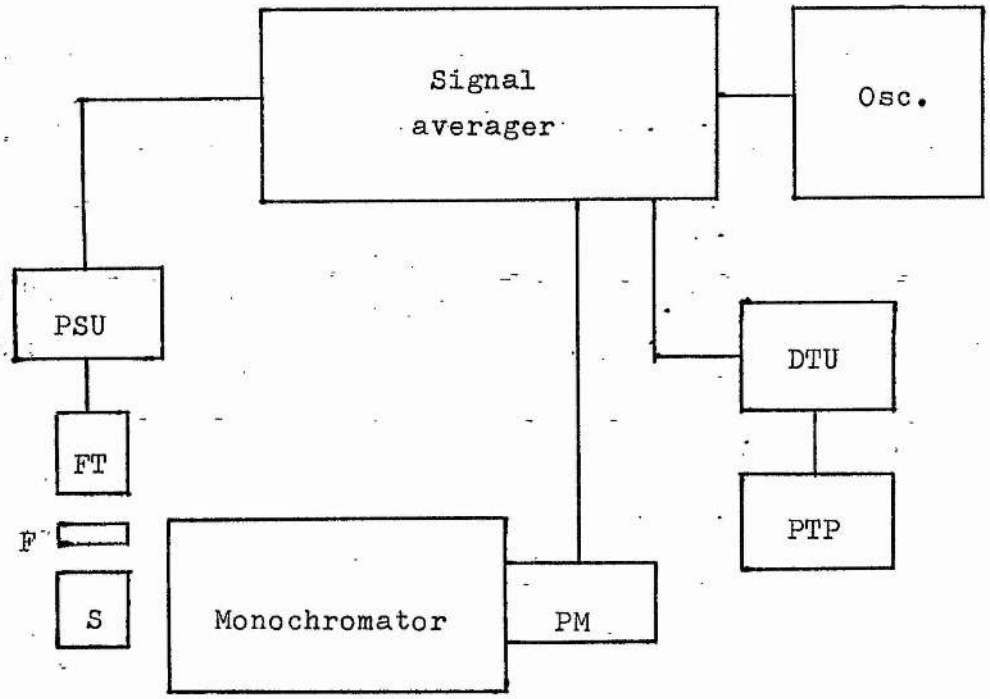

Signal averager - Data Laboratories Ltd., 200 point averager DL 102; FT - flash tube with flash duration $< 50\mu s$; PSU - power supply for FT, energy variable from 0.1 to 10 J; F - ultraviolet pass filter, Ox 1 or Ox 2 glass; S - sample cell, 90^{o} viewing; monochromator - Hilger Watts Monospek 1000; PM - photomultiplier, EMI 9526; Osc. - monitoring oscilloscope; DTU - Solartron data transfer unit; PTP - Facit 4070 paper tape punch.

Schematic diagram of the lifetime measurement apparatus

Figure 2.6

$1/t \rightarrow 0$, $X_{(t)} \rightarrow B \exp(-t/Z)$, thus giving values of B and Z.

(b) Operation

The delay before, sweep time, delay after, and the sampling cycle controls of the signal averager were preset depending on the intensity and lifetime of the sample. Information about averages, temperature, sweep time, and delay were manually punched onto the paper tape before the data stored in the averager were transferred. The rate of output from the signal averager, and the rate of sampling by the digital transfer system were adjusted such that 50 values were transferred during the output sequence.

(c) Program LIFETIME

This program performs a least squares regression analysis of points 7 to 37 in the data set, and obtains a best straight line relationship between the natural logarithm of the fluorescent intensity and time. On the basis of the slope of the line, the program calculates half and exponential lifetimes, and the difference and percentage difference between calculated and experimental intensities from which the percentage standard deviation from true exponentiality is determined. All this data is output on a line printer along with the number of averages performed, sample temperature, sweep time, and delay before. LIFETIME was written by Dr. C. R. S. Dean in association with Dr. T. M. Shepherd.

2.7. Determination of quantum yields

Absolute quantum yields have important practical value in:

i) analytical determinations, e.g. of purity;[4]

ii) calculation of thresholds for laser action;[15]

iii) judging the suitability of materials as wavelength shifters, or as energy donors;[4,16]

iv) study of non-radiative processes, for correlation of calculated luminescence lifetimes with those observed;[17]

v) making assignments of electronic transitions.[18]

To determine quantum yield directly, it is necessary to compare the rate of absorption of exciting light with the total rate of emission of fluorescence at all wavelengths and in all directions - in principle simple, but in practice difficult. A review by Demas et al.,[19] brings together information on various techniques for measuring quantum yields, and points out the advantages and disadvantages of each method.

(a) Relative quantum yields in solution

Many lanthanoid β-diketoenolate complexes tend to dissociate in organic solvents, especially at low concentrations, of say $\leq 10^{-5}$ mol dm^{-3}. The exact nature of the species present at these concentrations is unknown, and as a consequence, quantum yields have been determined at relatively high concentrations, i.e. ca. 10^{-2} mol dm^{-3}, where dissociation is known to be slight.

Front face illumination using the MPF-2A is used to obtain values of peak heights under identical conditions. The peak heights are measured from uncorrected emission spectra obtained

by illuminating the sample at or near the absorption maxima. The solid sampler was adapted to hold a 1 mm pathlength cell, (see Figure 2.7).

2.8. Molecular weight determinations

Molecular weight determinations are obtained using a Mechrolab Vapour Pressure Osmometer Model 301A. This system consists of two principle units, the sample chamber assembly containing the various elements of the osmometer, and the control unit containing a Wheatstone bridge, a null indicator, and a heater input control circuit.

Drops of pure solvent and solution are suspended on the thermistor beads, side by side in a closed chamber saturated with solvent vapour. As the pure solvent drop is in equilibrium with the pure solvent atmosphere of the sample chamber, the rates of evaporation and condensation are equal. However, the solution drop is not at equilibrium due to the lowered vapour pressure of a solution, and there is a net gain in solvent due to condensation. The result is a gain in heat at the solution thermistor with the resultant temperature difference between the two drops producing a potential difference. The potential difference generated is applied to the Wheatstone bridge circuit, and the resistance change necessary to bring about no net flow of charge is measured. As the vapour pressure lowering is a colligative property of solutions, the changes in resistance can be related to the concentrations of solute.

A calibration curve for the instrument can be constructed by plotting the $\Delta R/C$ values against C for a series of standard

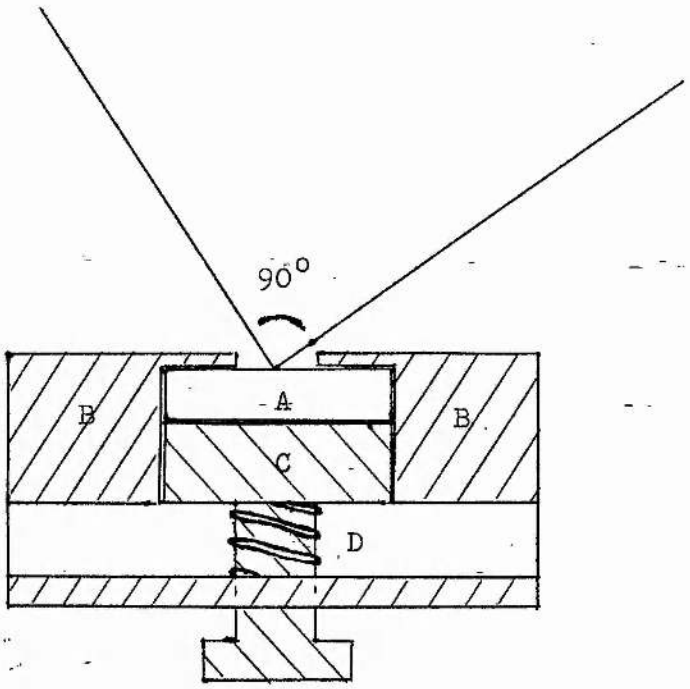

A. Sample cell. B. Positioning block. C. Pressure plate.

D. Spring load.

Adapted solid sampler accessory

Figure 2.7

solutions of known solute; where ΔR is the change in resistance, and C is the concentration. The concentrations of unknown solutes can then be read directly from the calibration curve.

The instrument was calibrated using benzil in the various organic solvents at 310K. Concentrations, and hence number average molecular weights, were obtained from the $\Delta R/C$ against C plots.

2.9. Nuclear magnetic resonance

N.m.r. spectra were measured using Varian EM-360 and HA-100 instruments.

The EM-360 is a 60 MHz instrument and was used for obtaining initial spectra for comparative purposes. The HA-100 is a 100 MHz system and was used for obtaining spectra of greater resolution than could be obtained from the EM-360. It was also used in conjunction with its variable temperature facility for investigation of the kinetics of lanthanoid complex interactions.

For greater resolution of one particular sample, a 220 MHz spectrum was obtained from the Physical Chemistry Measurements Unit, Harwell, England.

References

Chapter 2.

1. A. Job et al., Compt. Rend., 157 (1913) 50.
2. R.C. Young, Inorg. Syntheses, 2 (1946) 25.
3. D.D. Perrin et al., Purification of Laboratory Chemicals, Pergamon Press, Oxford, 1966.
4. C.A. Parker, Photoluminescence of Solutions, Elsevier, 1968.
5. R. Arganer et al., Fluorescence Analysis, Dekker, 1970.
6. J.F. Ireland, Ph.D. Thesis, St. Andrews, 1972.
7. C.R.S. Dean, unpublished work.
8. H.V. Drushel et al., Anal. Chem., 35 (1963) 2166.
9. P. Byron et al., Talanta, 15 (1968) 714.
10. B. Smaller et al., J. Chem. Phys., 43 (1968) 922.
11. W.R. Ware, Creation and Detection of the Excited State, Dekker, 1971.
12. E. Gaviola, Z. Physik, 35 (1926) 748.
13. E. Gaviola, Ann. Physik, 81 (1926) 681.
14. J.B. Birks, Photophysics of Aromatic Molecules, Wiley-Interscience, 1970.
15. P.P. Sorokin et al., J. Chem. Phys., 48 (1968) 4726.
16. J.G. Calvert et al., Photochemistry, Wiley, 1966.
17. S.J. Strickler et al., J. Chem. Phys., 37 (1962) 814.
18. F.E. Lytle et al., J. Amer. Chem. Soc., 91 (1969) 253.
19. J.N. Demas et al., J. Phys. Chem., 75 (1971) 991.

Chapter 3

Rates of Energy Transfer as determined by Change in Lifetime and Relative Quantum Yield

3.1. Choice of solvent and ultraviolet absorption

Ethanol was initially considered for use in the investigation of inter-molecular energy transfer between tris-(acetylacetonato)-lanthanoid complexes. However, it was noticed that a precipitate formed soon after the solutions of the various complexes were prepared. The ultraviolet spectra of these solutions were compared qualitatively after various time intervals and changes in both the positions and the strengths of the absorption were noted. Further investigation revealed that an isobestic point is formed, and the wavelength of maximum absorption of the apparent product of the reaction corresponds to that of acetylacetone.

Quantitative measurements of the absorptivities of the two bands against time were made using the data transfer system previously described for spectra correction, but attempted analysis of the data was unsuccessful in elucidating the kinetics of the proposed hydrolysis reaction.

Since it was found difficult to preserve ethanol in a sufficiently dry state over the length of time required for the investigations, several other alcohols were tried, and n-butanol was selected as the most suitable.

The ultraviolet spectra of the lanthanoid complexes were measured and the molar absorption coefficients computed at 290 nm. The value found for each complex and its ratio (r) with respect to that of $Tb(aa)_3.3H_2O$ are set out in Table 3.1

Compound	Molar extinction coefficient	Ratio
$Pr(aa)_3.3H_2O$	29870	0.868
Nd "	38100	1.108
Sm "	35100	1.020
Eu "	33100	0.962
Gd "	36365	1.057
Tb "	34400	1.000
Dy "	41900	1.218
Ho "	39100	1.137
Er "	34320	0.998
Yb "	41130	1.196

Molar extinction coefficients for $Ln(aa)_3.3H_2O$ at 290 nm, and the ratios compared to $Tb(aa)_3.3H_2O$.

Table 3.1

3.2. Energy transfer in mixed complexes

Dawson et al[1] reported the quantum efficiency of Tb^{3+} phosphorescence, Φ_{Tb}, in terbium acetylacetonate to be 0.19, following ligand excitation of an ethanolic solution at 296K. During the investigations, $Ln(aa)_3.3H_2O$ - (Ln = Pr, Nd, Sm, Eu, Gd, Tb, Dy, Er, and Yb) - were examined in n-butanol solution at 293K, and, with the exception of the terbium complex, no measurable Ln^{3+} emission was obtained when the ligand absorption band was irradiated. The corrected emission spectrum of $Tb(aa)_3.3H_2O$ in n-butanol solution over the range 470 to 630 nm is shown in Figure 3.1. The various bands in the emission spectrum of $Tb(aa)_3.3H_2O$ are due to radiative transitions from the Tb^{3+} $^5D_4$ level to members of the ^7F multiplet, the most intense occurring with the $^5D_4$ to $^7F_5$ transition at 547.5 nm. The decay of the $^5D_4$ level population after excitation was measured and found to be exponential within experimental error. The exponential lifetime at 293K was estimated to be 790 μs, with a standard deviation of $\pm$ 2.1%, and was constant over the concentration range 10^{-4} to 10^{-2}mol dm^{-3}.

Solutions of constant complex concentration were prepared using mixtures containing known ratios of terbium to lanthanoid acetylacetonates, $Tb_xLn_{(1-x)}(aa)_3.3H_2O$, in n-butanol at 293K. The quantum efficiencies of Tb^{3+} phosphorescence were measured relative to a 100% $Tb(aa)_3.3H_2O$ solution at the particular concentration. Simultaneously the lifetimes of the Tb^{3+} phosphorescence at 547.5 nm, i.e. $^5D_4$ to $^7F_5$ transition, of the solutions were measured.

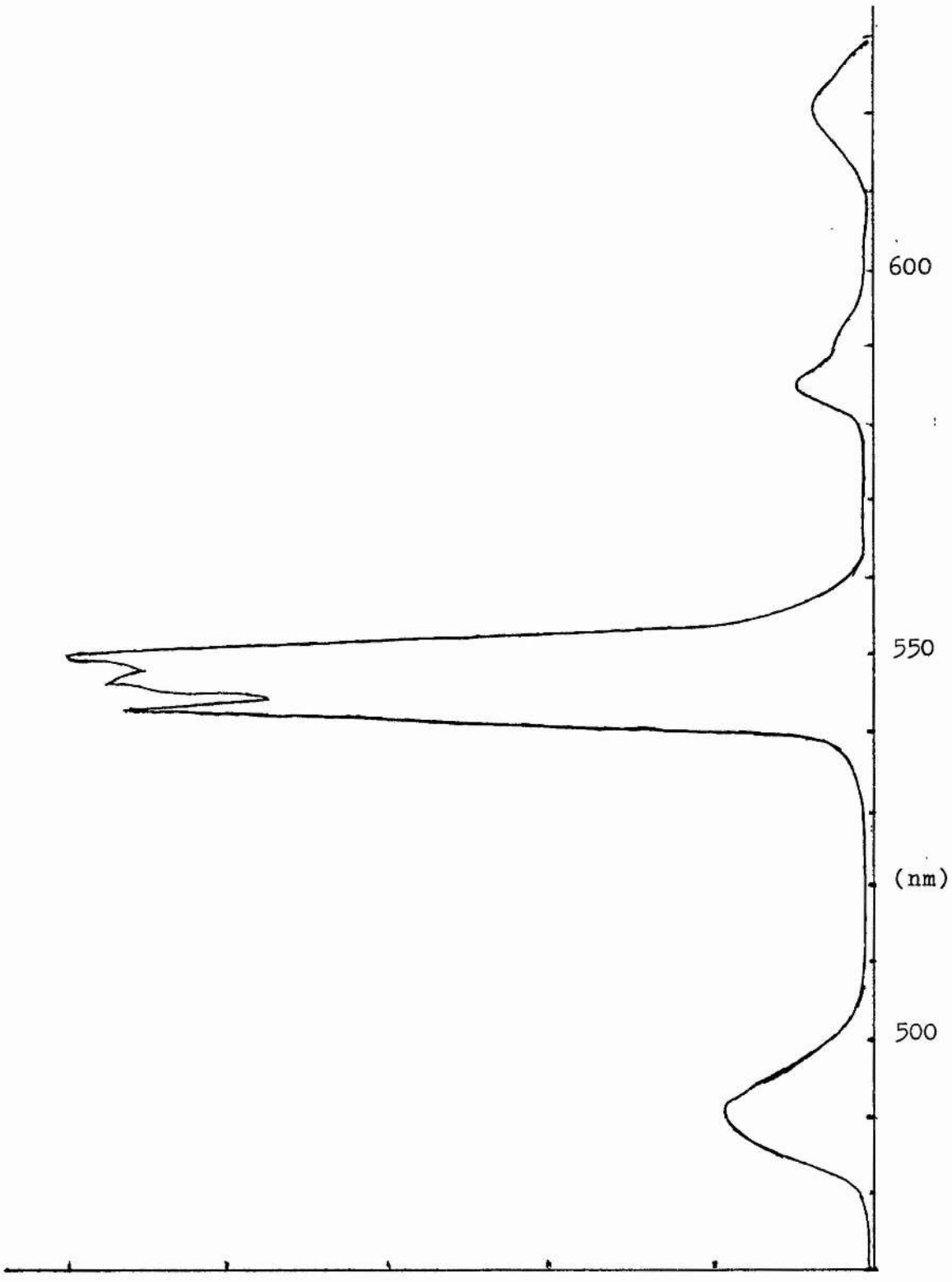

Corrected emission spectrum of $Tb(aa)_3 \cdot 3H_2O$ at 293 K

Figure 3.1

(a) Lifetime of Tb^{3+} phosphorscence in solutions of mixed complexes

In all cases examined, with the exception of Ln = Gd and Yb, the lifetime of the $^5D_4$ level decreased with increasing concentration of the added lanthanoid acetylacetonate. Since the $^5D_4$ level at 20.5×10^3 cm^{-1} lies some 5.0×10^3 cm^{-1} below the lowest ligand excited state, the triplet at 25.2×10^3 cm^{-1}, energy transfer from the $^5D_4$ to the excited ligand levels of $Ln(aa)_3.3H_2O$, both intra- and inter-molecularly, is improbable. Transfer of energy to the Ln^{3+} ion levels is supported by the constant τ obtained with Gd^{3+} and Yb^{3+}. The Gd^{3+} ion has no excited levels lower than ca. 32.0×10^3 cm^{-1}, the $^6P_{7/2}$, and the Yb^{3+} has only one f-f excited state, the $^7F_{5/2}$, lying at ca. 10.0×10^3 cm^{-1}; the former precludes transfer and the latter indicates that transfer is unlikely to be efficient. The negative results also confirm that the ligand excited levels are not involved, as these, to a good approximation, are independent of the nature of the Ln^{3+} ion.

At a total complex concentration of 5.0×10^{-3} mol dm^{-3}, the decrease in the lifetime in the presence of added lanthanoid acetylacetonate obeyed the relationship:

$$\tau_o/\tau_{(Ln)} = 1 + K[Ln]; \qquad \cdots\cdots \quad 3.1$$

where, τ_o is 790 μs, the lifetime of $Tb(aa)_3.3H_2O$ solution in the absence of added lanthanoid acetylacetonate; $\tau_{(Ln)}$ is the lifetime in the presence of added lanthanoid acetylacetonate, at concentration [Ln]; and K is the constant for any given lanthanoid complex. The results are set out in Table 3.2, with some typical plots shown in Figure 3.2. The corresponding values of K and the rate constants, k, for the bimolecular transfer process

Compound	K (dm^3 mol^{-1})	k (dm^3 mol^{-1} s^{-1})
$Pr(aa)_3 \cdot 3H_2O$	370	$4.7 \pm 0.3 \times 10^5$
Nd "	390	4.9 "
Sm "	390	4.9 "
Eu "	260	3.3 "
Gd[a] "	4	$0.05 \pm 0.2 \times 10^5$
Dy "	40	0.5 "
Ho "	160	2.0 "
Er "	120	1.5 "
Yb[a] "	4	0.05 "

a. No significant decrease in lifetime detected.

Total complex concentration is 5×10^{-3} mol dm^{-3}.

Stern-Volmer quenching constants, K, and bimolecular rate constants, k, of intermolecular energy transfer from $^5D_4(Tb^{3+})$ to excited levels of Ln^{3+} ions in the acetylacetonate complexes in n-butanol solution at 293 K

Table 3.2

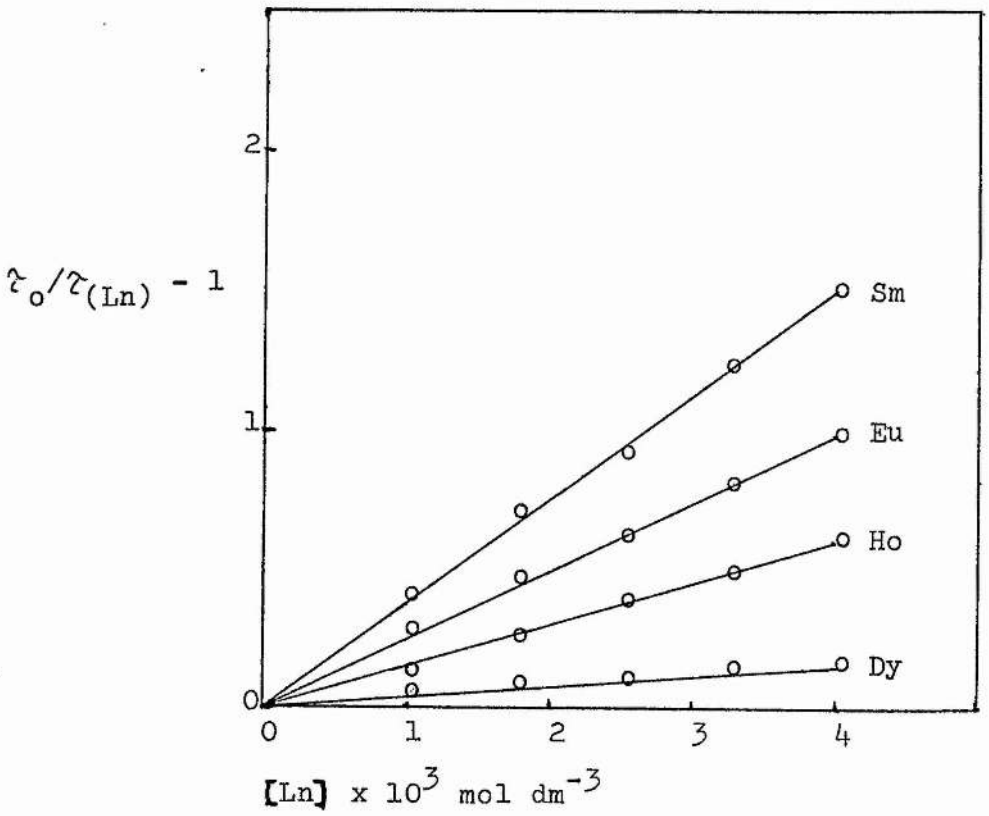

Typical plots of $(\tau_o/\tau_{(Ln)}) - 1$ against [Ln] at 5 x 10^{-3} mol dm^{-3} total concentration of $Tb_xLn_{1-x}(aa)_3 \cdot 3H_2O$ in n-butanol at 293 K

Figure 3.2

$^5D_4(Tb^{3+}) \rightsquigarrow Ln^{3+}$,

where, $k = K/\tau_o$, are given in Table 3.2.

The decrease in the Tb^{3+} $^5D_4$ lifetime has also been determined at total complex concentrations of 10^{-2}, 2.5×10^{-3}, and 1.25×10^{-3} mol dm^{-3} using Ln = Nd, Sm, Eu, and Ho, and found to obey Equation 3.1. The latter cases showed no significant change in K from that obtained at 5.0×10^{-3} mol dm^{-3}, but the former, which is close to the solubility limit of the complexes in n-butanol, gave values of K - 290 (Nd), 320 (Sm), 210 (Eu), and 140 (Ho) dm^3 mol^{-1} - which were lower, indicating a transfer rate which is apparently less in more concentrated solution.

The values of k obtained are considerably lower than the calculated diffusion rate constant, k_D, of n-butanol at 293K, where, using the approximation, $k_D = 8RT/2000\eta$, with η = 294.8 dyne s cm^{-2} (= 3.3×10^9 dm^3 mol^{-1} s^{-1}). For comparison, 'bare' ion energy transfer rate measurements in dimethyl sulphoxide solution have been reported by Chrysochoos and Evers[3], and Antipenko and Ermolaev[4] with values of $2.2 \pm 0.4 \times 10^3$ dm^3 mol^{-1} s^{-1} for $Tb^{3+} \longrightarrow Eu^{3+}$ ions in the former case, and 2.7×10^3 and 10^4 dm^3 $mol^{-1}s^{-1}$ for $Tb^{3+} \longrightarrow Ho^{3+}$ and $Tb^{3+} \longrightarrow Nd^{3+}$ respectively, in the latter case, at 293K.

The transfer rate constants for the chelated systems are significantly higher than those obtained for the 'bare' ions in DMSO, but are at least four orders of magnitude lower than that expected for diffusion control, and vary in magnitude by less than a factor of five except for Gd, Dy, and Yb.

The donor (Tb^{3+}) and acceptor (Ln^{3+}) ion transitions are Laporte forbidden, as they arise from changes within the 4f electronic configuration. The donor transition, $^5D_4 \longrightarrow {}^7F_n$,

and many of the acceptor transitions, e.g. (Eu^{3+}) $^5D_n \longrightarrow {}^7F_0$, where, n = 0 or 1, are also spin-forbidden. (Further, the lanthanoid ion absorption bands have relatively narrow bandwidths, as a consequence of the very effectively shielded 4f orbitals.) The forbidden nature of the transitions results in the absorption bands having molar extinction coefficients which are usually less than 5 mol^{-1} cm^2.

The radiationless transfer may occur by:

a) a Coulombic (Forster type[5]) mechanism involving multipole interaction; and/or,

b) an electron exchange (Dexter type[6]) mechanism.

The Forster equation may be written in the form:

$$k_D(r)_A\tau_D = \text{constant} \times r^{-6} \times \int_0^\infty f_D(\bar{\nu})\xi_A(\bar{\nu})\,d\bar{\nu}/4 \qquad \ldots\ldots 3.2$$

where, $k_D(r)_A$ is the transfer rate constant at distance r between donor and acceptor, τ_D is the donor lifetime, $f_D(\bar{\nu})$ is the donor fluorescence yield, and $\xi_A(\bar{\nu})$ is the acceptor molar extinction coefficient, i.e. the integral quantifies the overlap between D and A.

The transfer rate constant, k, for singlet-singlet spin-allowed transfer between organic molecules can exceed 10^{11} dm^3 $mol^{-1}s^{-1}$, the donor lifetimes usually being of the order of 10^{-8}s, leading to typical values of $k\tau$, i.e. the Stern-Volmer quenching constant, K, of ca. 10^3 dm^3 mol^{-1}.

In view of the low absorption of the lanthanoid ions and the possible restrictions on overlap imposed by the narrow bandwidths, the value of the integral term in Equation 3.2. is likely to be several orders of magnitude lower for Ln - Ln ion transfer than for singlet-singlet transfer. The values of

K found experimentally for the lanthanoid-lanthanoid ion transfers are in several cases greater than 10^2 dm^3 mol^{-1} which is considerably greater than would be predicted on the basis of the above considerations; and it is unlikely therefore that coulombic transfer is significant despite the relatively long Tb^{3+} donor lifetime.

In contrast, the electron exchange mechanism is governed by the less restrictive Wigner's spin selection rule and is spin allowed for $Tb^{3+} \rightsquigarrow Ln^{3+}$ transfer. Also, the absorption coefficient of the acceptor is not rate determining and providing that there is some overlap of the donor emission and acceptor absoption, transfer may occur if the lanthanoid ions are in close proximity to one another. It is therefore more probable that the observed intermolecular energy transfer is due to an electron exchange mechanism.

No obvious correlation was found between the rate constants, k, and the degree of overlap expected between the Tb^{3+} emission and the possible Ln^{3+} acceptor levels. This suggests that the rate determining step in this system is not the electron exchange interaction.

(b) Lifetime of Tb^{3+} phosphorescence in the solid state of mixed complexes

Since close physical proximity is necessary for transfer to occur by an electron exchange mechanism a simple model for the energy transfer in solution is that the approach of the Tb^{3+} donor ion and the Ln^{3+} acceptor ion has a minimum distance imposed by the size of the undissociated complexes, i.e.

ca. 0.7 nm. The low transfer rate constants may then be due to the low effeciency of the electron exchange mechanism between the shielded f-orbitals over this distance. However, if this approach is correct, then if the distances between the lanthanoid ions are fixed e.g. at ca. 0.7 nm in the crystalline state, the transfer rate constants in the mixed crystals, $Ln_x\ Tb_{(1-x)}(aa)_3\ 3H_2O$ should be at least those found in solution.

The $Tb^{3+}\ ^5D_4$ lifetime was measured in crystalline $Eu_x\ Tb_{(1-x)}(aa)_3\ 3H_2O$ with x = 0, 0.1, 0.3, and 0.5. The plot of the values obtained is shown in Figure 3.3.

The values obtained do not satisfy the Stern-Volmer relationship Equation 3.1, but assuming the density of the mixed crystal to be 1.5, a value of $K = 0.3\ dm^3\ mol^{-1}$ is obtained as x tends to zero, which is three orders of magnitude lower than for the n-butanol solution of the system.

The model suggested is shown to be too simple by the marked difference in the transfer rates between the solid state and solution. The observed transfer rates in solution indicate that the lanthanoid ions probably approach one another more closely than 0.7 nm, and in this the nature of the solvent is likely to be important.

(c) Relative quantuum yields of Tb^{3+} phosphorescence in solutions of mixed complexes

The measurements of the $Tb^{3+}\ ^5D_4$ lifetime only give information on intermolecular energy transfer from the $^5D_4$ level; and other intermolecular energy transfer processes may occur in solution, for example, between the ligand excited states

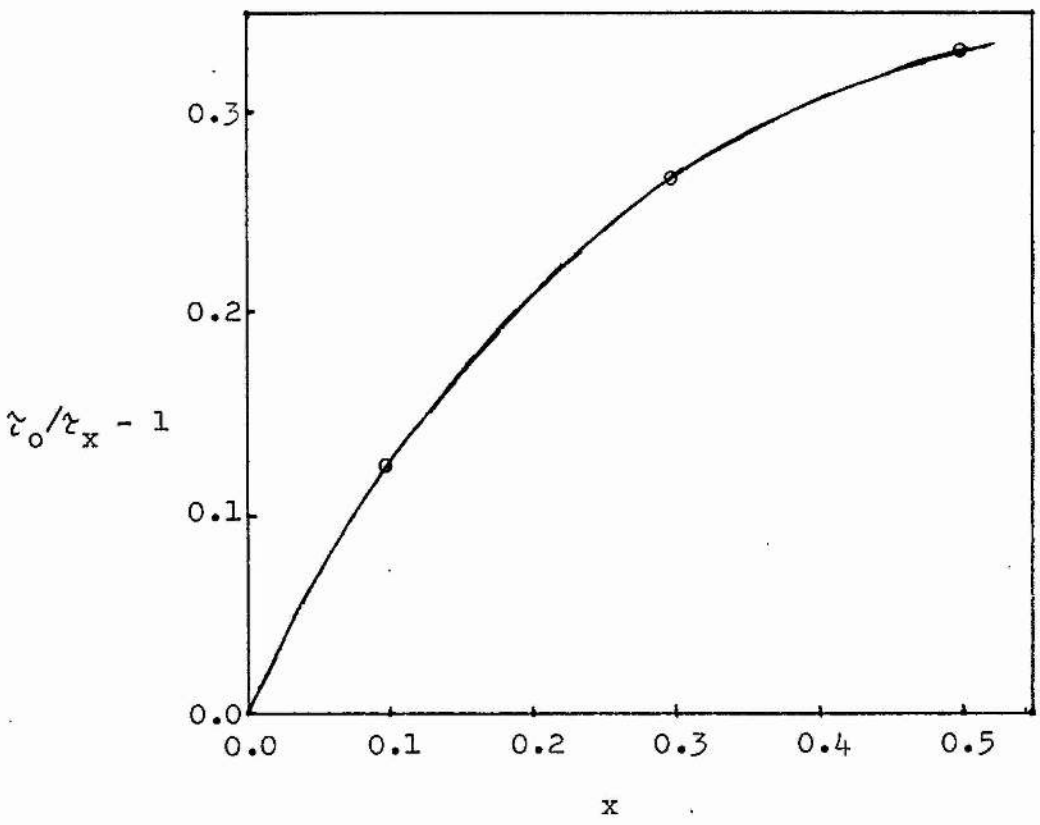

Plot of $(\tau_o/\tau_x) - 1$ against x in the mixed crystals, $Eu_xTb_{1-x}(aa)_3 \cdot 3H_2O$ at. 293 K

Figure 3.3

or a ligand excited state and a lanthanoid ion level. If a net population or depopulation of excited ligand or ion levels of the Tb^{3+} acetylacetonate (other than $^5D_4$) results from one or more of these processes, then the Tb^{3+} phosphorescence yield will be affected provided the levels involved are part of the radiative process at some stage.

The Tb^{3+} phosphorescence yield depends on $\tau_{(Ln)}$ due to the interaction of the Tb^{3+} $^5D_4$ and Ln^{3+} ion levels previously discussed, and in the absence of intermolecular population or depopulation of the higher excited states -

$$\phi_o/\phi_{(Ln)} = \tau_o/\tau_{(Ln)} = R_{(Ln)} \quad \ldots\ldots \quad 3.3$$

should be obeyed, where, ϕ_o is the Tb^{3+} phosphorescence yield in the absence of quencher, and $\phi_{(Ln)}$ the Tb^{3+} yield in the presence of (Ln).

For solutions of constant total lanthanoid complex concentration, the ratio $R_{(Ln)}$ may be determined by:

$$R_{(Ln)} = I_o x/I_{(Ln)}(x + r(1-x)) \quad \ldots\ldots \quad 3.4$$

where, I_o and $I_{(Ln)}$ are the measured phosphorescence outputs in the absence and presence of added lanthanoid complex respectively, x is the mole fraction of Tb^{3+} present, and r is the ratio of the absorbances of the Ln^{3+}/Tb^{3+} complexes at the excitation wavelength λ.

The phosphorescence ratio $R_{(Ln)}$ was measured in n-butanol solutions of total complex concentration 5×10^{-3} mol dm^{-3} at 293K on addition of $Ln(aa)_3.3H_2O$, where, Ln = Pr, Nd, Sm, Eu, Gd, Dy, Ho, Er, or Yb. Within experimental error, all the $R_{(Ln)}$ values were the same as the $\tau_o/\tau_{(Ln)}$ values, with the exception of Pr and possibly Eu. The $R_{(Pr)}$ values were consistently higher than the corresponding $\tau_o/\tau_{(Pr)}$, indicating that intermolecular energy transfer occurs to the Pr^{3+} complex from an

excited state of the Tb^{3+} complex other than the $^5D_4$ level.

If there is only one additional energy transfer step, then the equation:

$$R_{(Ln)}\tau_{(Ln)}/\tau_o = 1 + K'[Ln] \quad \ldots\ldots 3.5$$

should be obeyed, where, K' is the Stern-Volmer quenching constant for the second process.

In Figure (3.4.) the linear plot of $(R_{(Pr)}\tau_{(Pr)}/\tau_o) - 1$ shows that the Tb^{3+} phosphorescence results agree with the presence of a further intermolecular energy transfer step with $K' = 110\ dm^3\ mol^{-1}$.

The phosphorescence ratio has been measured in solutions of total complex concentration 10^{-2} mol dm^{-3}, where Ln = Nd, Sm, Eu, or Ho. At this higher concentration deviations between $R_{(Ln)}$ and the corresponding $\tau_o/\tau_{(Ln)}$ values occurred in all cases, but obeyed Equation 3.5; the values of K' are given in Table 3.3. In this transfer process it is unlikely that the acceptor levels are the ligand singlet or triplet levels, as they are virtually similar for all the lanthanoid complexes considered. The variations in K' with different acceptor complexes therefore indicates that the Ln^{3+} ion levels are involved. With the transfer leading to a decrease in the Tb^{3+} phosphorescence, the donor state must be involved in the intramolecular energy transfer in the terbium complex, and lie above the $^5D_4$ level.

The only Tb^{3+} ion level, apart from the ^7F multiplet, to lie at lower energy than the triplet of the acetylacetonate ligand is the $^5D_4$. However, the $^5D_3$ and $^5D_2$ Tb^{3+} ion levels occur at lower energy than the lowest excited singlet state of the acetylacetonate ligand (see Figure 3.5).

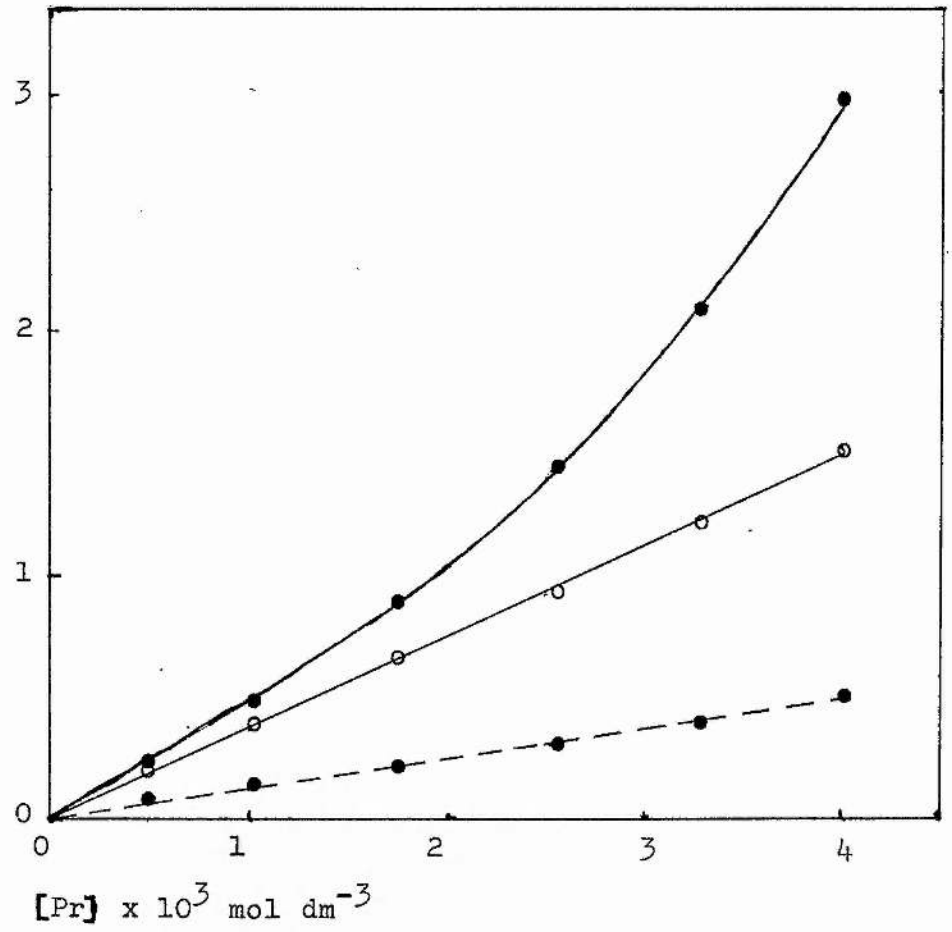

Plots of $(\phi_o/\phi_{(Pr)}) - 1$, (—●—●—●—); $(\tau_o/\tau_{(Pr)}) - 1$, (—o—o—o—); and, $(R_{(Pr)}\tau_{(Pr)}/\tau_o) - 1$, (– ●– ●– ●– →) against [Pr] in n-butanol solution at 293 K and total complex concentration 5 x 10^{-3} mol dm^{-3}

Figure 3.4

Compound	K' ($dm^3\ mol^{-1}$)
$Pr(aa)_3 \cdot 3H_2O$[a]	110
Nd "	22
Sm "	11
Eu "	52
Ho "	11

a. Obtained with total lanthanoid complex concentration of 5×10^{-3} mol dm^{-3}; other values obtained at 10^{-2} mol dm^{-3}.

Stern-Volmer quenching constants, K', of the additional energy transfer process from terbium acetylacetonate to other lanthanoid acetylacetonate complexes in n-butanol solution at 293 K.

Table 3.3

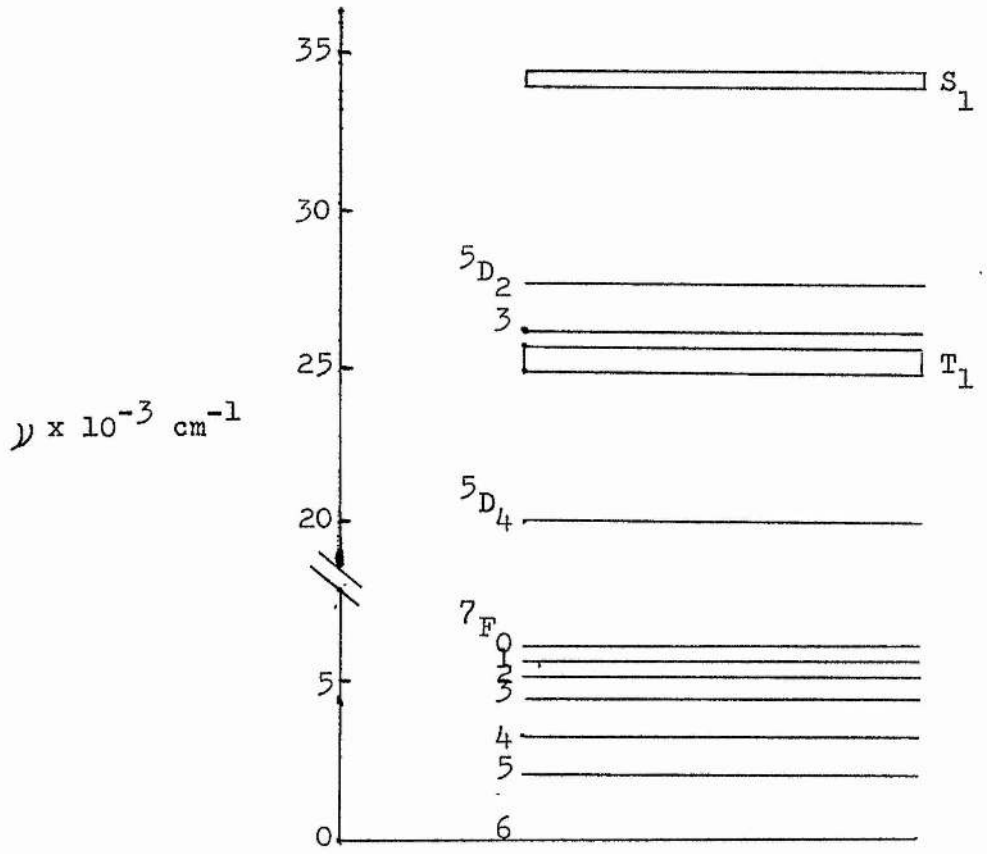

Schematic diagram of the energy levels of $Tb(aa)_3 \cdot 3H_2O$ in n-butanol solution. Not all the higher Tb^{3+} levels are included

Figure 3.5

The intramolecular energy transfer mechanism leading to lanthanoid ion phosphorescence in β -diketoenolates is generally thought to follow the route: ground state singlet $\longrightarrow$ excited state singlet (S_1) $\longrightarrow$ triplet (T_1) $\longrightarrow$ excited lanthanoid ion level, as set out in the introduction. The higher excited Ln^{3+} ion levels other than the $^5D_4$ do not appear in this scheme, and the only potential donor levels are the excited state singlet and triplet levels.

The very low phosphorescence yield of S_1 indicates that $\tau_{(S_1)}$ is probably $< 10^{-9}$s, and reported rate constants for $T_1 \rightsquigarrow {}^5D_4$ in a series of Tb^{3+} complexes with aromatic acids indicate that $\tau_{(T_1)} < 10^{-9}$s. Taking the values of K' as in Table 3.3. implies that the rate constants, k', are greater than 10^{10} dm^3 mol^{-1} s^{-1} for transfer from either S_1 or T_1 to the Ln^{3+} levels. As the transfer in both cases is spin-forbidden, for the coulombic transfer, rate constants exceeding that of diffusion control are improbable. Kleinerman[7] has suggested that intramolecular transfer occurs from the excited singlet state of the ligand direct to the lanthanoid ion levels. If this is so then the Tb^{3+} $^5D_3$ level is a potential donor, and providing the lifetime of this level is less than 10^{-7}s, then a diffusion controlled electron exchange transfer could account for the observed values of K'.

References

Chapter 3.

1. W.R. Dawson et al., J. Chem. Phys., 45 (1966) 2410
2. S.P. Sinha, Complexes of the Rare Earths, Pergamon Press, London, 1966.
3. J. Chrysochoos et al., Chem. Phys. Letters, 20 (1973) 174.
4. B.M. Antipenko et al., Opt. Spectr., 26 (1969) 415.
5. Th. Forster, Disc. Faraday Soc., 27 (1959) 7.
6. D.L. Dexter, J. Chem. Phys., 21 (1953) 836.
7. M. Kleinerman, J. Chem. Phys., 51 (1969) 2370.

Chapter 4

Molecular Weight and Proton Magnetic Resonance Studies

4.1. Effect of solvent on Tb^{3+} $^5D_4$ lifetime and energy transfer

To investigate the effect of varying the solvent on the transfer rate, the Tb-Eu and Tb-Sm systems of the tris-acetylacetonate-trihydrate complexes were employed because of their relatively high values of k, the bimolecular transfer rate constant. The decay of the Tb^{3+} $^5D_4$ level was found to be exponential in all solvents tried, within experimental error, both before and after addition of the Ln^{3+} quenching complexes. The lifetime, τ_o, (in the absence of quencher) varies significantly among the different solvents, indicating that the solvent influences the non-radiative decay rate of the $^5D_4$ level.

The total molar concentration of the acetylacetonate complexes was constant at 5×10^{-3} mol dm^{-3}, and in all solvents where a significant decrease in the lifetime was observed, the relationship:

$$\tau_o/\tau_{(Ln)} = 1 + K_{SV}[Ln] \quad \ldots\ldots \quad 4.1$$

was obeyed; where, τ_o is the lifetime of the Tb^{3+} $^5D_4$ level in the absence of quencher complex, $\tau_{(Ln)}$ is the lifetime of the Tb^{3+} $^5D_4$ level in the presence of quencher complex at concentration [Ln], and K_{SV} is the Stern-Volmer quenching constant. A Stern-Volmer relationship is consistent with a bimolecular reaction mechanism, and the corresponding bimolecular rate constants, k, are derived from:

$$k = K_{SV}/\tau_o \quad \ldots\ldots \quad 4.2$$

for each solvent. (See Table 4.1)

Intermolecular energy transfer occurred in all polar solvents tried, excepting pyridine and dimethyl sulphoxide (DMSO); while in non-polar solvents, e.g. benzene and carbon tetrachloride, no significant decrease in lifetime was obtained. The absence of a measurable decrease in lifetime for the systems indicates that the rate of intermolecular energy transfer in these solvents occurs at least two orders of magnitude lower than in, for example, acetone.

The solvent dependent behaviours of the Tb-Ln systems can be grouped in three sets:

a) no significant decrease in the lifetime for the non-polar solvents such as benzene;

b) a marked decrease in the lifetime for one sub-set of polar solvents, i.e. acetone, acetonitrile, benzonitrile, and ethylene glycol; and,

c) no significant decrease in the lifetime for the other sub-set of polar solvents, i.e. pyridine, and DMSO.

On examination of the bulk solvent properties of the solvents, e.g. dielectric constant, viscosity, and refractive index, no obvious correlation with the transfer rate constants was found. The emission spectra of $Tb(aa)_3.3H_2O$ have been established for the various solvents after ligand excitation at ca. 300 nm, but no obvious correlation has been found with variation in the spectral profiles. (The variations are due to changes in the microsymmetry of the Tb^{3+} ion caused by crystal field splittings of the $^5D_4 \longrightarrow {}^7F_6$, $^7F_5$, and $^7F_4$ transitions. These effects are small since the 4f electrons are well shielded.)

Solvent	τ_o^a (μs)	k_{Eu} (dm^{-3} mol^{-1} s^{-1})	k_{Sm} (dm^{-3} mol^{-1} s^{-1})
n-butanol	790	3.3×10^5	4.9×10^5
acetone	800	3.3 "	3.9 "
acetonitrile	930	3.3 "	3.8 "
benzonitrile	825	3.3 "	1.3 "
ethylene glycol	695	1.5 "	1.5 "
pyridine	595	b	b
dimethyl sulphoxide	650	b	b
carbon tetrachloride	830	b	0.1 "
benzene	900	b	0.1 "

a. Tb^{3+} $^5D_4$ lifetime in absence of quencher; estimated error $\pm$ 15 μs.

b. No significant decrease in Tb^{3+} $^5D_4$ lifetime.

Bimolecular rate constants, k, of intermolecular energy transfer from the Tb^{3+} $^5D_4$ level of $Tb(aa)_3.3H_2O$ to lanthanoid ion levels of the corresponding Eu and Sm complexes in various solvents at 293 K. The values were determined from the observed decreases in the Tb^{3+} $^5D_4$ lifetime

Table 4.1

4.2 Molecular weight dterminations and p.m.r. studies of some lanthanoid complexes in solution

The intermolecular energy transfer is expected to be dependent on the nature of the lanthanoid species in solution. This aspect has given rise to conflicting reports in the literature. Blitz[1] reported some lanthanoid acetylacetonates to be dimeric in non-polar solvents; later Freed et al.[2] proposed that dimers occurred in benzene solutions of the europium complex, and that a monomer-dimer equilibrium could exist; Moeller et al.[3], in conflict, reported that the complexes were monomeric in both benzene and carbon tetrachloride; Dutt et al.[4], produced results which indicated the presence of a monomer in acetone, and more complicated behaviour in dioxane; while Pope et al.[5], significantly recognising the hydrated nature of the complexes, found that the trihydrates in benzene gave apparent molecular weights of between 500 and 700.

In view of the inconsistencies in the literature, attempts were made to clarify the nature of the species in solutions of various solvents by number average molecular weight determinations, and by proton magnetic resonance spectroscopy.

(a) Vapour pressure osmometric studies of some lanthanoid complexes

Vapour pressure osmometric studies of several lanthanoid acetylacetonate complexes in benzene solution at 310K were undertaken, and the results recorded in terms of $\bar{n}$, the average number of monomer units (i.e. $Ln(aa)_3.3H_2O$) per solute molecule. In all cases (see Table 4.2) $\bar{n}$ was greater than unity, indicating that association occurs. The data in Table 4.2 shows a decrease in the value of $\bar{n}$ with increasing atomic number, especially in the second

'Compound'[a]	$\bar{n}$[b]
$Pr(aa)_3.3H_2O$	2.03 ± 0.15
Nd "	1.89 "
Sm "	2.06 "
Eu "	2.03 "
Gd "	2.12 "
Tb "	1.98 "
Dy "	1.76 "
Ho "	1.93 "
Er "	1.87 "
Yb "	1.67 "
$Lu(aa)_3.2H_2O$	1.66 "

a. 0.01 mol dm^{-3} with respect to monomer.

b. $\bar{n}$ is average number of monomers per solute molecule.

Molecular weight measurements of $Ln(aa)_3.nH_2O$ in benzene solution at 310 K

Table 4.2

half of the series. This may be interpreted as a decrease in the degree of association, and has a parallel in the structures of complexes of the light and heavy lanthanoids in the crystalline state: $Pr(fod)_3.3H_2O$[6]; fod is $(C_3H_7.CO.CH.CO.^tBu)^-$, is dimeric containing 8-coordinate Pr^{3+} ions bridging two β-diketoenolate and one oxygen atom, whereas the lutetium[7] complex contains 7-coordinate Lu^{3+} ions with a single H_2O oxygen bridge; $Pr(dpm)_3$[8], dpm is $(^tBu.CO.CH.CO.^tBu)^-$, is dimeric with two ligand oxygen atoms bridging 7-coordinate Pr^{3+} ions, while the erbium complex[9] is monomeric.

An alternative interpretation of the data is that dimerisation is complete throughout the series but that the hydration of the dimer complex decreases with increasing atomic number, and the subsequent release of water molecules into the system lowers the $\bar{n}$ value.

Molecular weight measurements of $Ln(aa)_3.3H_2O$ complexes, where Ln = Sm, Eu, and Tb, in the polar solvents acetone and acetonitrile, were made under the same conditions as for benzene. The mean values of $\bar{n}$ produced were 1.47 ± 0.2 for acetone and 1.67 ± 0.2 for acetonitrile. In these cases also there is the possibility of either of the interpretations for the deviation from $\bar{n} = 2$ corresponding to dimer. To resolve these uncertainties, structure determination from p.m.r. spectra was attempted.

(b) <u>P.m.r. studies of some lanthanoid complexes in non-polar solvents</u>

The proton magnetic resonance (p.m.r.) spectrum of $Lu(aa)_3.2H_2O$ recorded at 100 MHz and 278K in C_6D_6 solution, shows two broad resonances at 1.90 and 1.57, and further downfield another two

broad resonances at 5.27 and 4.90. (All figures quoted are p.p.m. downfield of tetramethylsilane.) These two sets have an intensity ratio of 6:1; i.e. the areas under the resonances at 1.90 and 1.57 combined, compared with the areas under the resonances at 5.27 and 4.90 combined, are in the ratio of 6 to 1. With this in mind, the high field resonances (1.90 and 1.57) are assigned to the ligand methyl protons, and the low field resonances (5.27 and 4.90) to the C3-protons of the ligand.

On varying the concentration of the solution between 0.02 and 0.08 mol dm^{-3} (based on $Lu(aa)_3.2H_2O$), the ratio between the components of the high and low field resonances, i.e. 1.90/1.57 and 5.27/4.90, remains constant at 2:1. This implies that there is probably only one complex species present in solution.

Since benzene solutions are unsuitable for temperature work below ca. 278K because of the limiting factor of freezing point, the spectrum in toluene-d_8 was obtained and compared with that in C_6D_6. Since they are almost identical - 1.89, 1.57, 5.26, 4.89 compared with 1.90, 1.57, 5.27, 4.89 - toluene-d_8 was used for the low- temperature and C_6D_6 for the high-temperature studies of $Lu(aa)_3.2H_2O$ in a typical non-polar solvent.

P.m.r. spectra of the complex were determined at 10K intervals over the range 278K to 383K in C_6D_6 solutions and 213K to 303K in toluene-d_8. Representative spectra are shown in Figure 4.1. Where the integration of the components of the high and low field resonances was possible, the components were found to be in the ratio of 2:1. The implication is that a single species is present in the solution over the temperature range 213K to 383K.

Further observations of the resonance profiles at various temperatures show a pattern. At 213K, the four resonances are:

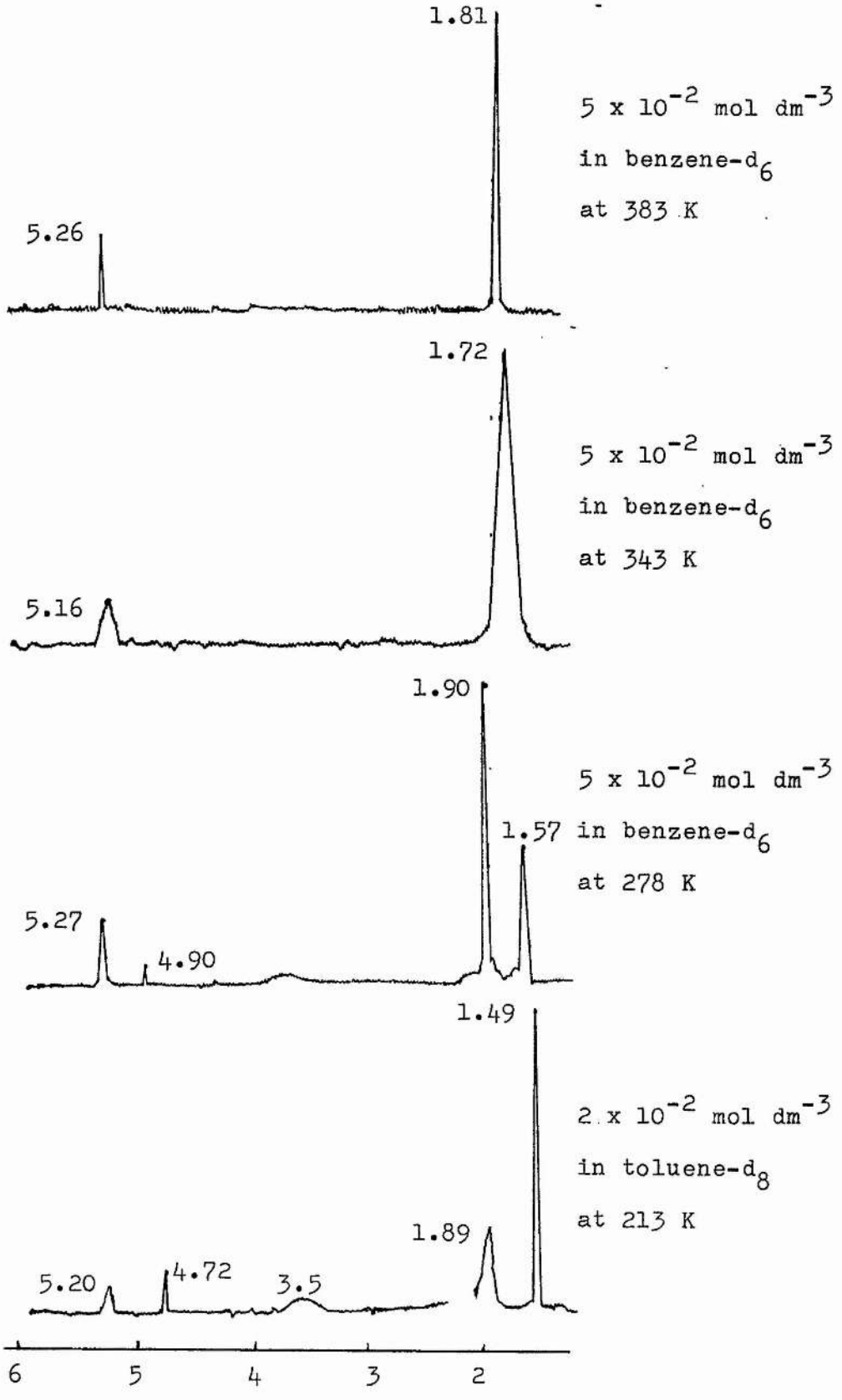

The 100 MHz n.m.r. spectra (in ppm) of $Lu(aa)_3.2H_2O$ in solution

Figure 4.1

i) 5.20 (broad), ii) 4.72 (narrow), iii) 1.89 (broad), and, iv) 1.49 (narrow). As the temperature increases to ca. 293K, (i) and (iii) narrow, and (ii) and (iv) shift downfield. Above ca. 293K, all the resonances broaden with increasing temperature, until at ca. 343K, (i) and (ii), as well as (iii) and (iv) coalesce at 5.16 and 1.72 respectively. Further increase in the temperature narrows both bands, and shifts them downfield, so that at 383K their values are 5.26 and 1.81 respectively.

A broad resonance at ca. 3.5 was attributed to the water molecules, on the basis of the integration. The resonance is discernable only at the lower temperatures, but its position was not dependent on temperature. On this basis, it is suggested that the water molecules are exchanging between equivalent sites on the complex.

As resonances (i) and (iii) broaden with increasing temperature, it is possible that further structural information may be gained if resolution can be obtained. Since it was not practicable to lower the temperature by the required amount, a p.m.r. spectrum was obtained at 220 MHz and 203K in toluene-d_8 solution. Resonance (iii) was found to split into two equal intensity broad peaks at 1.89 and 1.82, as shown in Figure 4.2. The foregoing data can be interpreted as indicating that a single complex species exists in these non-polar solvents, most probably the dimer, $Lu_2(aa)_6 \cdot 4H_2O$. From the temperature dependence of the spectral profiles, it may be inferred that ligand exchange is occurring intramolecularly at two different rates dependent on the complex sites involved. The first is fast, with a coalescence temperature of greater than 213K, and the second is much slower, with a coalescence temperature of ca. 340K, both with respect to 100 MHz.

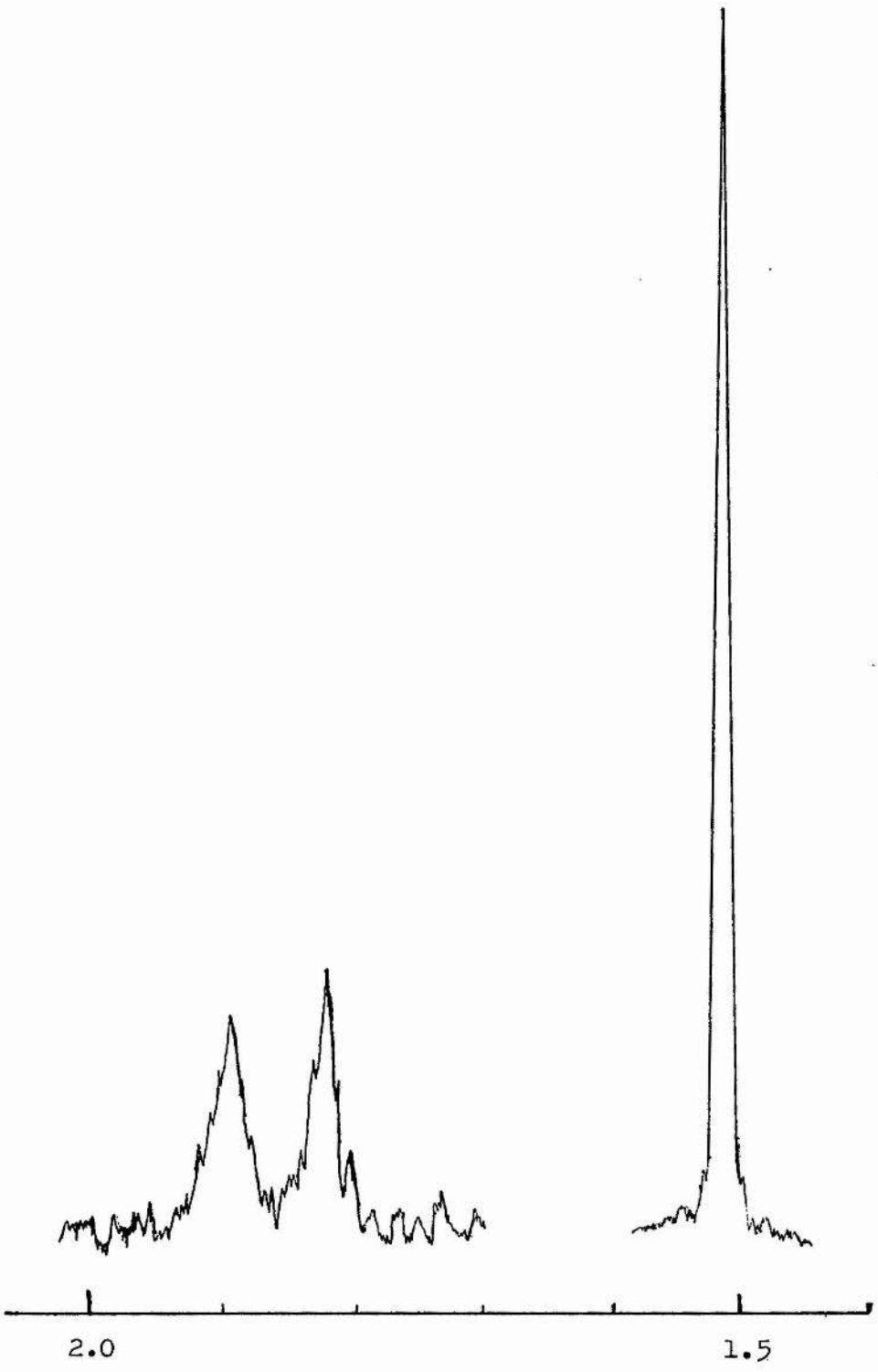

The 220 MHz n.m.r. spectrum (in ppm) of $Lu(aa)_3.2H_2O$ in toluene-d_8 solution at 203 K showing the ligand methyl resonances

Figure 4.2

The information regarding the inequivalencies of the methyl protons obtained from the 220 MHz p.m.r. spectrum is not sufficient of itself to enable the assignment of a definite structure. A tentative proposal, based on the 1:1:1 ratio found, is a structure involving four ligand oxygens bridging the metal atoms in a dimer; see Figure 4.3. This structure does not give a role to the water molecules originally present as part of the monomers. The information available at present does not debar them from assuming a bridging role, and the structure shown may be altered appreciably.

(c) P.m.r. studies of some lanthanoid complexes in polar solvents

In line with the scope of the molecular weight determinations, p.m.r. spectra of the lutetium complex were recorded in acetone-d_6. The temperature range covered was 183K to 363K at 100 MHz. At 183K the resonances are single and narrow, occurring at 1.78 and 5.38. The former is assigned to the methyl- and the latter to the C3-protons on the basis of the integrated areas of the resonance peaks. Above 183K, additional peaks appear at 1.89 and 5.40, with intensities in the ratio 6:1, enabling their assignment to a second set of ligand methyl- and C3-protons to be made. These resonances increase in intensity relative to the initial signals with increase in temperature, and eventually the two sets coalesce at ca. 303K. Further increase in temperature results in line narrowing, and at 363K the resonances occur at 1.86 and 5.39.

The dependence of the relative areas of the two sets of ligand methyl- and C3-proton resonances on temperature is in contrast to the behaviour found in the non-polar solvents, benzene and toluene.

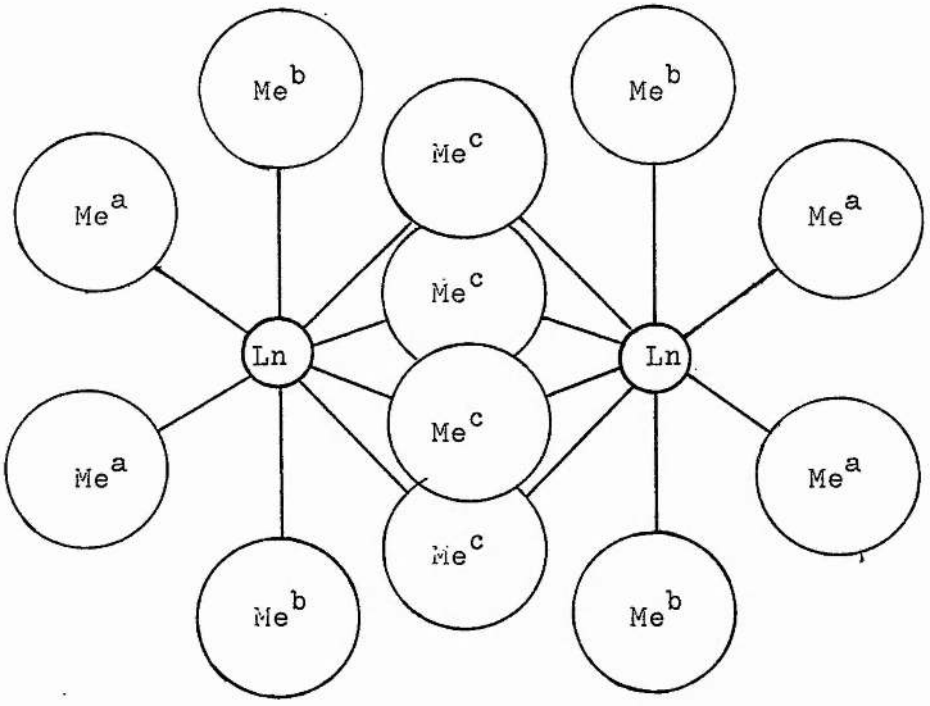

Ratio of protons on methyl groups a, b, and c is 1:1:1.

A schematic of a possible structure for the dimeric species existing in non-polar solvent solution

Figure 4.3

It is assumed that the high and low field components of the methyl- and C3-proton resonances can be attributed to dimeric and monomeric species respectively, and that these species are in equilibrium in the acetone-d_6 solution. Then, by integrating the appropriate resonances in the spectrum, the relative concentrations, and hence the equilibrium constant, may be obtained for the situation:

Monomer + monomer $\rightleftharpoons$ Dimer; and, ... 4.3

$K = (\text{Dimer})/(\text{Monomer})^2$. 4.4

The C3-proton resonances in the spectra were not sufficiently resolved, in general, to be useful for integration purposes, and the methyl proton resonances only were used for the equilibrium constant estimations.

For the temperature range 233K to 293K using a solution of concentration 0.128 mol dm^{-3}, based on $Lu(aa)_3.2H_2O$, the integrations were assumed to be representative of the concentrations of the dimer and monomer, and values of K were calculated at 10K intervals.

Plotting lnK against 1/T gives a linear relationship, which supports the idea of a monomer-dimer, or stoichiometrically equivalent, equilibrium. On varying the concentration between the limits 0.04 and 0.14 mol dm^{-3}, values of K were obtained which were similar within experimental error. A least squares regression line of the lnK versus 1/T plot, gives values of ΔH^o = -28.2 $\pm$1.5 kJ mol^{-1} and ΔS^o = -74.5 $\pm$4.5 J K^{-1} mol^{-1} for the equilibrium. It is unlikely that the tetramethylsilane (ca. 3%) used as an internal reference in the acetone solution, and that concentration rather than activity terms were used in determining K, will lead to large errors in the derived enthalpy and entropy values.

A broad single resonance for the water molecules was also observed for acetone solutions. In contrast to the benzene/toluene case, the resonance is both concentration and temperature dependent. For example, in the 0.128 mol dm^{-3} acetone solution, the resonance occurs at ca. 4.6 for temperature 183K and shifts to ca. 3.0 for temperature 293K. This is attributed to the water molecules exchanging rapidly between the acetone solvent and sites on the complex. It is probable that the complex sites are the more favoured position at the lower temperatures.

The coalescence point at ca. 303K is proposed as the exchange rate for the monomers and dimers, which is an intermolecular ligand transfer process. This is in contrast to the intramolecular ligand exchange in the benzene/toluene case. The corresponding process in the acetone solution cannot be detected in the spectra obtained for the temperature range examined. This implies either that the process does not occur, which is unlikely, or that it is very much faster than in the benzene/toluene case. The difference in rate proposed, suggests that there may be structural differences between the dimers formed in the two cases, i.e. the dimeric species formed is solvent dependent.

P.m.r. spectra were obtained of $Lu(aa)_3.2H_2O$ in both dimethyl sulphoxide (DMSO) and pyridine solutions at 303K. Single narrow resonances occurred at 1.78 and 5.33 for DMSO, and at 1.84 and 5.41 for pyridine. On the basis of intensity, the peaks are assigned to ligand methyl- and C3-protons respectively.

On adding either of these two solvents to benzene or acetone solutions of $Lu(aa)_3.2H_2O$, single resonances with values characteristic of the solvent added appear. This is interpreted as the formation of a monomeric species which is strongly solvated and has no tendency to form dimers.

References

Chapter 4.

1. W. Blitz, Annalen, 331 (1904) 334.
2. S. Freed et al., J. Amer. Chem. Soc., 63 (1941) 1079.
3. T. Moeller et al., J. Inorg. Nucl. Chem., 2 (1956) 164.
4. N. K. Dutt et al., Nature, 181 (1958) 1682.
5. G. W. Pope et al., J. Inorg. Nucl. Chem., 20 (1961) 304.
6. J. P. R. De Villiers et al., Acta Cryst., B27 (1971) 692.
7. J. C. A. Boeyens et al., J. Cryst. Mol. Struct., 1 (1971) 2971.
8. C. S. Erasmus et al., Acta Cryst., B26 (1970) 1843.
9. J. P. R. De Villiers et al., Acta Cryst., B27 (1971) 2335.

Chapter 5

Relative Quantum Yield Measurements as Indicators of the Monomer-Dimer Interactions

5.1 Introduction

The dimeric units of the lanthanoid tris acetylacetonate complexes have an attractive feature from the aspect of ion-ion energy transfer and that is the relative proximity of the metal ions.

In the crystalline state the ion-ion distance is 0.414 nm for $Pr(dpm)_3^1$ whereas the expected value for two touching monomeric units is ca. 0.7 nm; so that although the distances are not necessarily the same for the dimers proposed in solution, it can be predicted confidently that the metal-metal distance will be less than for the monomer-monomer case. This is particularly relevant in that the energy transfer between the lanthanoid acetylacetonates appeared to be a relatively short-range effect.

It has been shown that in benzene solution the lanthanoid complexes are, within experimental error, entirely dimeric. Mixed solutions of terbium acetylacetonate and another lanthanoid acetylacetonate should attain therefore an equilibrium of the type:

$$Tb_2(aa)_6.6H_2O + Ln_2(aa)_6.6H_2O \rightleftharpoons 2TbLn(aa)_6.6H_2O \quad \ldots\ldots \quad 5.1$$

in which mixed metal dimers exist. These mixed metal dimers would provide a very favourable situation for energy transfer from an excited Tb^{3+} ion to the Ln^{3+} ion due to the proximity of the metals.

It is proposed that a very rapid Tb^{3+} to Ln^{3+} energy transfer step occurs in the mixed metal acetylacetonate dimers, with a rate greater than 10^5 s^{-1}, and this is the predominant cause of the observed lanthanoid-lanthanoid energy transfer. With this proposal in mind, the three types of solvent behaviour can be examined: i.e. no transfer in non-polar solvents e.g. benzene; no transfer in one type of polar solvents e.g. pyridine; and, transfer in the other type of polar solvents e.g. acetone.

5.2 Relative quantum yield measurements of benzene type solutions

If no significant decrease in τ occurs in benzene solution on addition of europium or samarium acetylacetonate, the rate of 'monomer exchange' between dimers has to be slow in comparison to the excited Tb^{3+} lifetime of *ca.* 1 ms in the di-terbium dimer. The proposed rapid Tb^{3+} to Ln^{3+} energy transfer step in the TbLn dimers, and the slow 'monomer exchange' rate would result in the Tb^{3+} phosphorescence yield of the mixed dimer being near zero. This leaves the TbTb dimer as the species in solution responsible for the observed Tb^{3+} phosphorescence. The slow rate of 'monomer exchange' would prevent processes such as, in condensed form:

$TbTb^* + LnLn \rightleftharpoons TbLn^* + TbLn$; or, ... 5.2

$TbTb^* + TbLn \rightleftharpoons TbLn^* + TbTb$, ... 5.3

leading to any significant decrease in τ. (*-excited species)

Evidence supporting this explanation has been obtained by measuring the Tb^{3+} phosphorescence, ϕ, after mixing benzene solutions of terbium and europium acetylacetonates - see Figure 5.1. ϕ decreases and reaches a steady value after *ca.* 6 min, when the initial dimer concentrations are 2.5×10^{-3} mol dm^{-3}. This result corresponds with the attainment of equilibrium:

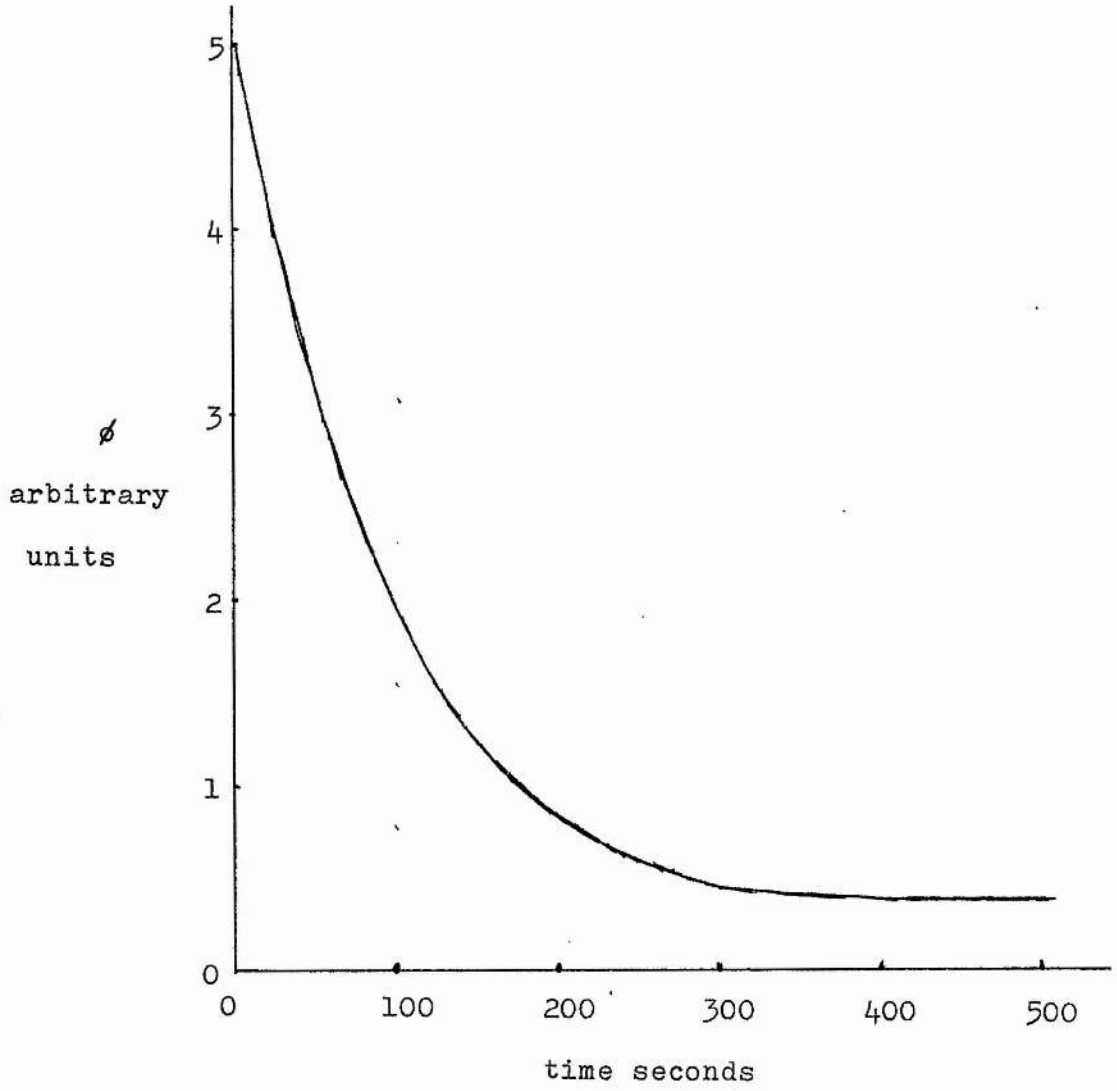

Relative Tb^{3+} phosphorescence yield, ø, after the mixing of 5 x 10^{-3} mol dm^{-3} benzene solutions of $Tb(aa)_3.3H_2O$ and $Eu(aa)_3.3H_2O$ at 293 K

Figure 5.1

$K = [TbEu]^2/[Tb_2][Eu_2]$, ... 5.4

and is consistent with the rate of 'monomer exchange' being $\gg \tau$. The equilibrium constant, K, was calculated from the value of $\phi_{initial}$ and ϕ_{final}; ϕ_{final} corresponding to the equilibrium value (assuming that the phosphorescence yield of the mixed metal dimer is zero). Several mixed solutions of differing concentrations have been investigated in this way and give values of K = ca. 400 for the TbEu case. The main sources of error in determining K are:

a) estimating the value of ϕ at time zero; and,

b) the error in determining the equilibrium value of ϕ, on which K is critically dependent, when $\phi_{equilibrium} \ll \phi_{initial}$. Problem (a) could be minimised by using apparatus which would ensure very rapid mixing.

The agreement, within experimental error, in K, derived from solutions of differing concentrations, confirm that the observed slow decrease in ϕ is due to the attainment of equilibrium, which is reached more slowly if the concentrations of the Tb_2 and Eu_2 dimers are lowered. Attempts to make a kinetic analysis were abandoned as the data did not yield to simple schemes.

Another significant point that was noted in this experiment was that with decreasing Tb^{3+} phosphorescence output after benzene solutions of terbium and europium complexes were mixed, it was possible to follow a corresponding increase from zero to a steady value in the Eu^{3+} red phosphorescence. This is notable in that the Eu_2 dimer does not give any measurable Eu^{3+} phosphorescence, and this has been attributed to the presence of a charge transfer band which interrupts the normal intramolecular energy transfer process. (See Chapter 6.) The increasing Eu^{3+} phosphorescence

thus gives direct evidence of a $Tb^{3+} \longrightarrow Eu^{3+}$ ion energy transfer step in the mixed metal dimer. Mixing experiments were also undertaken with other lanthanoid complexes in place of $Eu_2(aa)_6.6H_2O$. Where Ln = Pr, Nd, Sm, Dy, Ho, and Er, similar curves were obtained to that in Figure 5.1. In the case of Ln = Gd, and Lu, no change in $\emptyset$ occurred after the mixing, which is expected, as Gd^{3+} and Lu^{3+} ions do not have excited levels below or near the Tb^{3+} $^5D_4$ donor level at ca. 20.0×10^3 cm^{-1}; so that $Tb^{3+} \longrightarrow Lu^{3+}$ energy transfer cannot occur in those two cases.

From the curves obtained for concentrations of 5×10^{-3} mol dm^{-3} in benzene solution at 293K, it appears that the mean lifetime of the individual dimers is of the order of 1 min, which is longer than the Tb^{3+} excited state lifetime by four to five orders of magnitude.

5.3 Relative quantum yield measurements of acetone type solutions

Acetone and acetonitrile solutions differ from benzene solutions in that a considerable concentration of monomer exists in equilibrium with the dimer. In a mixed solution of terbium and one other lanthanoid acetylacetonate, therefore, three equilibria co-exist:

$Tb + Tb \rightleftharpoons Tb_2$; 5.5

$Ln + Ln \rightleftharpoons Ln_2$; and, ... 5.6

$Tb + Ln \rightleftharpoons TbLn$, ... 5.7

involving five different species - two monomers, and three dimers. Of the possible interactions which may occur under these circum-

stances, only those which bring an excited Tb^{3+} ion into close interaction with an Ln^{3+} ion as a TbLn dimer will tend to lower the observed Tb^{3+} ion lifetime. The simplest process of this type is the monomer-monomer reaction:

$$Tb^{*} + Ln \longrightarrow TbLn^{*}. \qquad \ldots\ldots 5.8$$

In addition there are the monomer-dimer reactions:

$$(a)\ TbTb^{*} + Ln \rightleftharpoons TbLn^{*} + Tb; \qquad \ldots\ldots 5.9$$

$$(b)\ Tb^{*} + Ln_2 \rightleftharpoons TbLn^{*} + Ln, \text{ or } TbLn + Ln^{*}; \text{ and,} \qquad \ldots\ldots 5.10$$

$$(c)\ Tb^{*} + TbLn \rightleftharpoons TbLn^{*} + Tb, \text{ or } Tb_2 + Ln^{*}. \qquad \ldots\ldots 5.11$$

It is unlikely that dimer-dimer reactions such as:

$$TbTb^{*} + LnLn \rightleftharpoons TbLn^{*} + TbLn, \qquad \ldots\ldots 5.12$$

are sufficiently rapid to make any significant contribution to the observed decrease in τ when the results in benzene solution are considered. No direct experimental evidence was found to indicate whether the predominant reaction mechanism, which allows Tb^{3+} ion quenching, is through the monomer-monomer reaction, or through the various monomer-dimer reactions.

In the monomer-monomer case, the rate of loss of energy, k_L, from the excited Tb^{3+} ions to the quenching Ln^{3+} ion may be approximated by:

$$k_L = k_{MM}[Ln]; \qquad \ldots\ldots 5.13$$

where, k_{MM} is the monomer-monomer reaction rate constant. Assuming that the nature of the lanthanoid ions do not have a marked effect on the reaction rates when the ions involved have such similar radii as:

Tb (0.0923 nm), Sm (0.0964 nm), and Eu (0.0950 nm),[2]

then for the monomer-dimer reactions:

$$k_L = k_{MD}([Ln_2] + [LnTb] + [Ln]), \qquad \ldots\ldots 5.14$$

where, k_{MD} is the monomer-dimer reaction rate constant.

In a mixture of terbium and another lanthanoid acetylacetonate:

$[Ln^{3+}] = 2[Ln_2] + [Ln] + [LnTb]$, ... 5.15

and therefore the derived expressions can be rewritten as:

$k_L = k_{MM} [Ln^{3+}] - 2[Ln_2] - [LnTb]$; and, ... 5.16

$k_L = k_{MD} [Ln^{3+}] - [Ln_2]$, respectively. 5.17

As the Stern-Volmer plots for the Tb^{3+} lifetime quenching by Ln^{3+} complexes were found to be linear with the total concentration of added lanthanoid complex, $[Ln^{3+}]$, and the lifetime decrease was independent of the Tb^{3+} ion concentration, monomer-dimer reactions would appear to predominate as the quenching mechanism. However, to state this more firmly would require accurate knowledge of the equilibrium constants for the processes. For a quenching mechanism in which the $Tb^{3+} \longrightarrow Ln^{3+}$ energy transfer is not the rate determining step, there may be an activation energy associated with the formation of the TbLn dimer, and the corresponding derived rate constants, k, should be temperature dependent, obeying, at least to a first approximation:

$k = A.\exp(-E/RT)$, ... 5.18

where E is the activation energy.

The rate constants, k, were determined at temperatures of 273K, 293K &323Kfor the systems Tb-Eu and Tb-Sm in n-butanol. The plots of lnk against 1/T (Figure 5.2) were linear, within experimental error, and indicated activation energies of 23.2 kJ mol^{-1} (Eu), and 23.0 kJ mol^{-1} (Sm).

A feature of the energy transfer rates from Tb^{3+} to the different lanthanoid ions is their similarity, in that they vary by a factor of ca. 3, with the exceptions of Gd^{3+}, Dy^{3+}, and Yb^{3+} and show a trend in decreasing with increasing atomic number. With the association to form the mixed dimer rather than

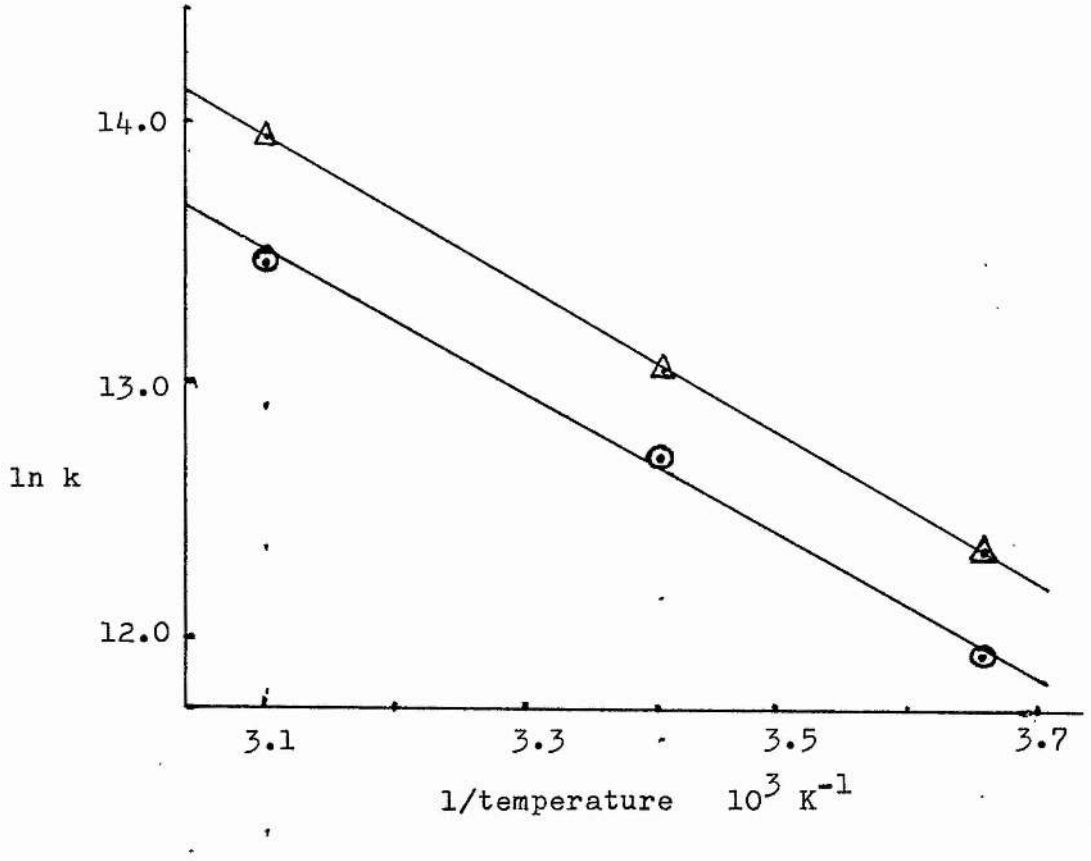

Plots of ln k against 1/T, where k = derived rate constant of intermolecular energy transfer between $Tb(aa)_3.3H_2O$ and $Ln(aa)_3.3H_2O$ in n-butanol solution. △, Ln = Sm, and ○, Ln = Eu

Figure 5.2

an electron - exchange mechanism being the rate controlling step for the energy transfer, a general similarity in the rate constants is to be expected. As further support, the equilibrium constants, K, derived from the mixing experiments show slight decreases with increasing atomic number, which could result from an increasing activation energy for the formation of TbLn dimers as the radii of the lanthanoid ions decrease towards the end of the series.

5.4. Relative quantum yield measurement of pyridine type solutions

The final general type of solvent behaviour was that found, for example, in pyridine solution. It was not possible to determine the number average molecular weights in either DMSO or pyridine solution by vapour pressure osmometry. However, from the proton magnetic resonance studies on $Lu(aa)_3.2H_2O$ in both solvents, it appears that the complex exists in a monomeric form; probably in a strongly solvated state. The absence of any decrease in the Tb^{3+} lifetime can be attributed to the lack of association of the complexes to form mixed dimers, due to the solvents strongly coordinative saturation of the lanthanoid ions. On adding pyridine to a benzene solution of europium and terbium acetylacetonates, the red Eu^{3+} phosphorescence disappeared and was replaced by the characteristic green phosphorescence of Tb^{3+}. The dimers initially in the benzene solution are dissociated to monomers by the increased stability given to the monomer complexes through coordinative saturation by the pyridine. The relatively low value of τ_0 in pyridine solution tends to confirm that the terbium species is different from those in benzene and acetone, for example.

References

Chapter 5.

1. C. S. Erasmus et al., Acta Cryst., B26 (1970) 1843.

2. T. Moeller, The Chemistry of the Lanthanons, p20, Reinhold, New York, 1963.

Chapter 6

Charge-Transfer Excited State in Tris(acetylacetonato) Europium(III)

6.1 Introduction

A comparison of the Eu^{3+} and Tb^{3+} ion energy levels with respect to the triplet energy level of the acetylacetonate ligand, see Figure 6.1, would lead to the conclusion that europium ion phosphorescence from the $Eu(aa)_3.3H_2O$ complex would be comparable in strength to that from the analogous terbium complex, on irradiation in the acetylacetonate absorption band at ca. 290 nm. However, both in the solid and liquid solution states, no Eu^{3+} phosphorescence is detectable, and Dawson et al.[1] have estimated the quantum efficiency, ϕ_{Eu}, of Eu^{3+} emission in methanol to be less than 0.002 on irradiating the ligand. In contrast, the analogous terbium complex quantum efficiency is 0.19[1].

Eu^{3+} phosphorescence arising from the $^5D_0$ level does occur on excitation of the higher Eu^{3+} levels - $^5D_1$, $^5D_2$, and $^5L_7$.

6.2 Results and discussion

The quantum efficiency, ϕ_{Eu}, of Eu^{3+} $^5D_0$ emission may be expressed as:

$$\phi_{Eu} = \phi_{IS}.\phi_{TM}.\phi_{C}.\phi_{R}, \qquad \ldots\ldots 6.1$$

where, ϕ_{IS} is the intersystem crossing efficiency of ligand singlet to ligand triplet, ϕ_{TM} is the ligand triplet to Eu^{3+} acceptor level transfer efficiency, ϕ_C is the efficiency of the cascade process from the Eu^{3+} acceptor level to the $^5D_0$ emitting

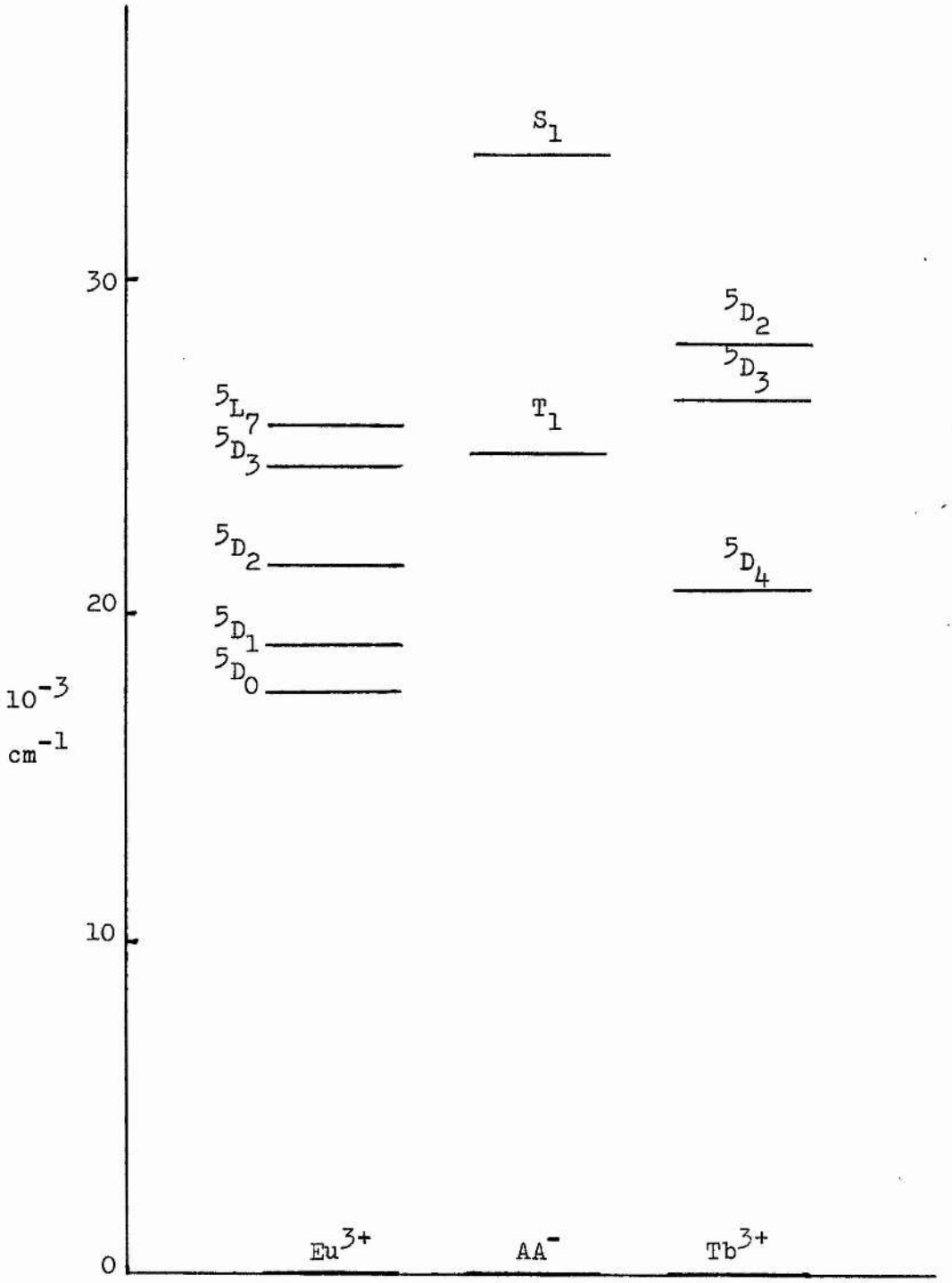

Energy levels of Tb^{3+}, Eu^{3+}, and the acetylacetonate anion

Figure 6.1

level, and, ϕ_R is the radiative efficiency of the $^5D_0$ level.

From the results reported by Dawson et al.[1], in methanol, $\phi_R = 0.18$, and ϕ_C for $^5L_7 \longrightarrow {}^5D_0 = 0.06$ and for $^5D_2 \longrightarrow {}^5D_0 = 0.33$. Therefore, assuming the energy transfer process involves $^5L_7$ to $^5D_0$ and $\phi_{Eu} < 0.002$, then, $\phi_{IS} \cdot \phi_{TM} < 0.2$, and is probably much lower since the ϕ_{Eu} value is an upper limit determined by the measurement technique employed. Hence the intersystem crossing and/or the ligand triplet, T, to Eu^{3+} energy transfer steps are much less efficient in the europium as compared with the terbium acetylacetonate.

The energies of the acetylacetonate π- and non-bonding orbitals are not expected to be especially sensitive to the particular lanthanoid ion. Absorption spectra of $Ln(aa)_3 \cdot 3H_2O$ in dry n-butanol solution confirm this. See Table 6.1. The absorption maxima at 290 $\pm$ 3 nm are assigned to the lowest energy $S_0 \longrightarrow S_{\pi,\pi^*}$ transition, and the unresolved shoulders at *ca.* 305 nm to the weaker symmetry forbidden $S_0 \longrightarrow S_{n,\pi^*}$ transition. See Figure 6.2. The spectra resemble that of $Al(aa)_3$ in ethanol solution, in which the $S_{\pi,\pi^*} - S_{n,\pi^*}$ energy difference has been estimated at *ca.* 2×10^3 cm^{-1}.

The maximum of the 0—0 band at 397 nm in the corrected ligand phosphorescence spectrum of $Gd(aa)_3 \cdot 3H_2O$ in ethanol solution at 77K establishes the energy of the lowest ligand triplet, T_{π,π^*}. This is in reasonable concurrence with previously reported values[2], and the energy is unlikely to vary significantly with a change in Ln^{3+}.

There is no evidence to suggest that any Ln^{3+} dependent variation in S_{π,π^*}, S_{n,π^*}, or T_{π,π^*} is directly responsible for the anomalous behaviour of the europium complex.

Ln	λ_{max} (nm)	log ε_{max}
Pr	291.5	4.53
Nd	291.5	4.58
Sm	291	4.59
Eu	289	4.57
Gd	289.5	4.57
Tb	289.5	4.55
Dy	289	4.62
Ho	288	4.59
Er	288	4.64
Yb	287	4.56

Acetylacetonate absorption maxima, λ_{max}, and molar extinction coefficients, ε_{max}, of $Ln(aa)_3 \cdot 3H_2O$ in dry n-butanol solution

Table 6.1

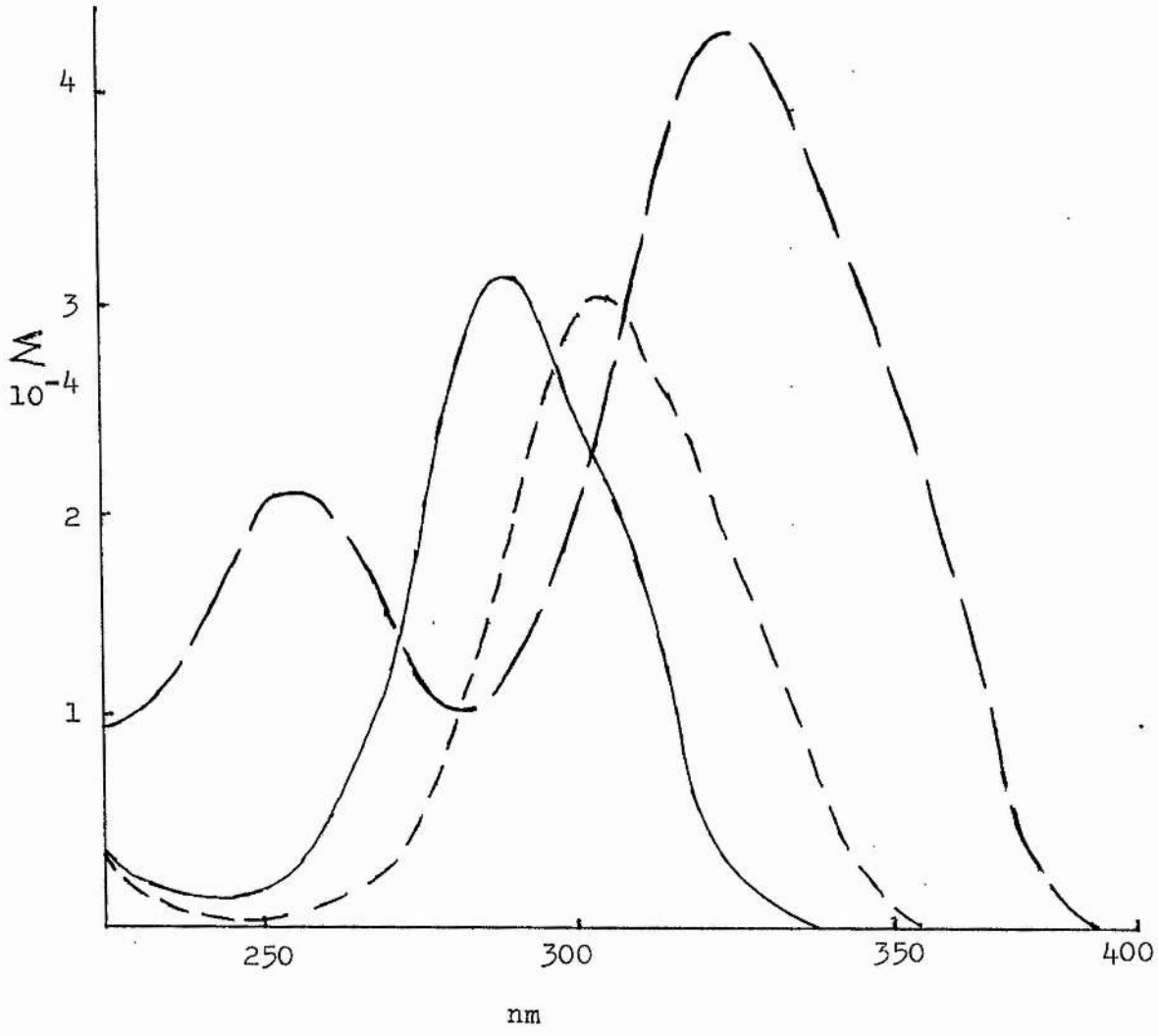

The absorption spectra of $Eu(aa)_3 \cdot 3H_2O$ (———), $Eu(hfaa)_3 \cdot 2H_2O$ (– – –), and $Eu(btfa)_3 \cdot 2H_2O$ (—— ——) in n-butanol solution

Figure 6.2

Closer examination of the absorption spectrum of the europium acetylacetonate complex brings to notice a low frequency absorption edge of relatively low intensity which extends into the visible — $\varepsilon_{360\ nm} = 205\ cm^2\ mol^{-1}$, $\varepsilon_{415\ nm} = 10\ cm^2\ mol^{-1}$. With the exceptions of Ho and Er which have relatively strong f-f absorption above 360 nm, the molar extinction coefficients of the other lanthanoid complexes examined are less than 15 $cm^2\ mol^{-1}$ in this region. The additional band is not resolved from the steep absorption edge of the ligand $\pi \rightarrow \pi^*$ and $n \rightarrow \pi^*$ transitions (Figure 6.3), but comparison with the spectra of the other lanthanoids indicates that λ_{max} is <u>ca.</u> 320 nm ($\varepsilon_{max} > 500\ cm^2\ mol^{-1}$), which is at lower energy than the S_{n,π^*}.

$Eu(dpm)_3$ has, like the acetylacetonate complex, a very low ϕ_{Eu} in the solid and solution states, whereas $Tb(dpm)_3$ is quite efficient. Here again examination of the absorption spectrum of $Eu(dpm)_3^3$, (dpm = $^tBu.CO.CH.CO.^tBu^-$), also finds long wavelength absorption — $\varepsilon_{350\ nm} = 560\ cm^2\ mol^{-1}$, $\varepsilon_{400\ nm} = 15\ cm^2\ mol^{-1}$ — which is absent in the corresponding $Tb(dpm)_3$ complex — $\varepsilon_{350\ nm} = 30\ cm^2\ mol^{-1}$.

It is proposed that the additional absorption in the europium complexes is due to ligand to metal charge transfer. Its occurrence at low energy in the Eu^{3+} cases is supported by the low reduction potential — $Eu^{3+}/Eu^{2+} = -0.35$ V in aqueous solution[4] — by comparison with the other tripositive lanthanoid ions.

Barnes[5] has reported charge-transfer, CT, absorption in the complexes of Eu^{3+} with NCS^- (346 nm), Br^- (320 nm), and Cl^- (276 nm) in ethanol solution. The europium complex CT bands lie

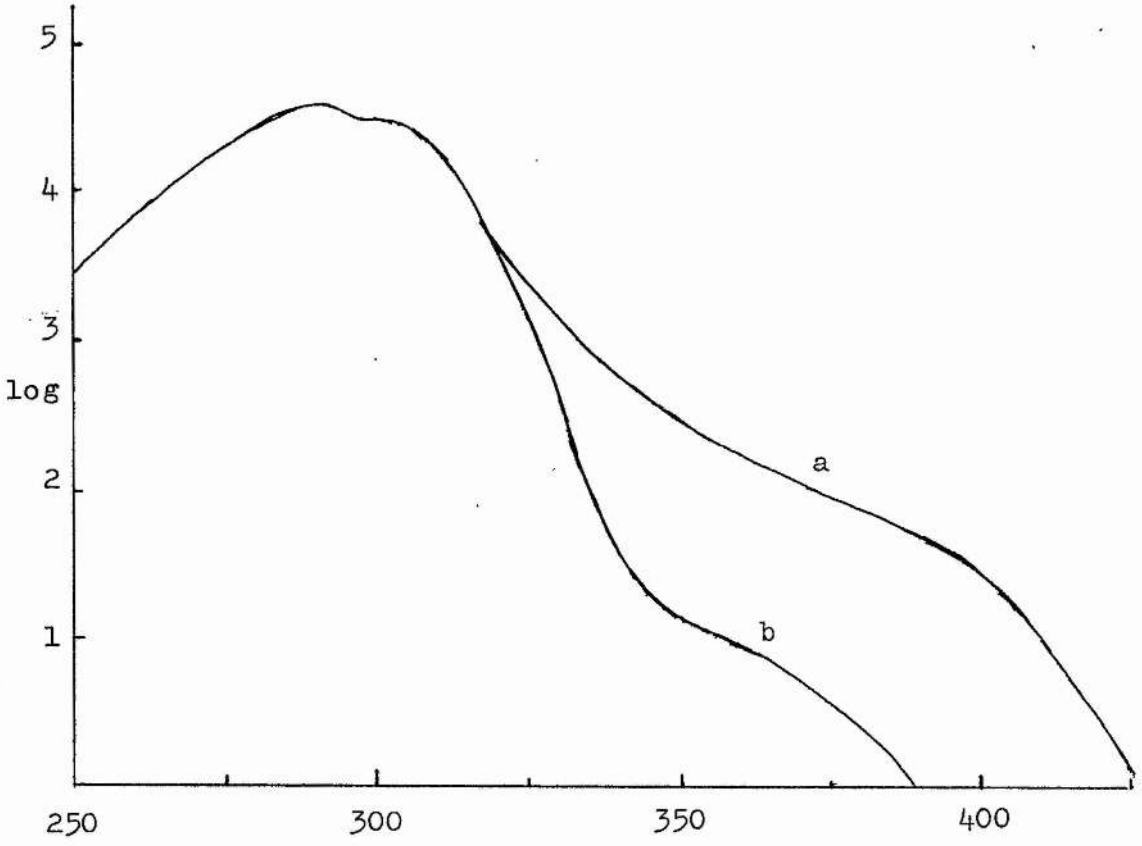

Absorption spectra of (a) $Eu(aa)_3 \cdot 3H_2O$, and (b) $Gd(aa)_3 \cdot 3H_2O$

Figure 6.3

$3 - 5 \times 10^{-3}$ cm^{-1} lower in energy than the corresponding complexes of Yb^{3+}, which is the next most readily reducible Ln^{3+} ion — Yb^{3+}/Yb^{2+} = 1.15 V in aqueous solution.[4] Similar long wavelength absorption bands have been observed in Eu^{3+} complexes of a series of substituted benzoic acids[6] and attributed to CT transitions. Absorption at ca. 245 nm in various Cu (β-diketoenolate)$_2$ complexes has been assigned as ligand to metal ion CT involving a non-bonding ligand electron.[7] The greater covalency of the Cu - ligand bonding may be largely responsible for the apparent inverted order - Cu^{2+}/Cu^{+} = + 0.153 V -[8] of the Cu^{2+} and Eu^{3+} CT transitions.

The very low ϕ_{Eu} of the acetylacetonate and dpm complexes may be associated with the presence of the low energy CT band. It is significant that many europium tris (β-diketoenolates) including, for example, Eu (hfaa)$_3$ $2H_2O$[9], (hfaa = $CF_3COCHCOCF_3^-$) and Eu (btfa)$_3$ $2H_2O$[10], (btfa = $CF_3COCHCOPh^-$), exhibit very efficient intramolecular energy transfer. In these particular cases the lower ligand singlet levels lie at lower energy than in the acetylacetonate complexes (Figure 6.2), and the corresponding CT transition presumably occurs above the S_{n,π^*} and perhaps also above the S_{π,π^*} state. It is suggested that in both the acetylacetonate and dpm europium complexes, an $S_{\pi,\pi^*} \longrightarrow S_{n,\pi^*} \longrightarrow$ CT process occurs where the rate of $S_{n,\pi^*} \longrightarrow$ CT exceeds the normal intersystem crossing rate, thus greatly reducing the ligand triplet yield.

An alternative explanation that the S_{n,π^*} intersystem crosses to a CT triplet state which undergoes rapid deactivation to the ground state is less satisfactory because it does not necessitate CT(singlet) $<$ S_{n,π^*} and might therefore be expected

to reduce ϕ_{Eu} in a wider range of europium complexes than observed. Haas et al.[11] have observed fluorescence in aqueous solutions of Eu^{3+}, following excitation in the CT band, from both the CT state and an excited state of Eu^{2+}. No corresponding fluorescence has been detected in the europium acetylacetonate complex in solution.

Investigations into the effect of adding KBr and KNCS to ethanolic solutions of hydrated $Eu(hfaa)_3$ and $Eu(btfa)_3$ showed that KBr has no significant effect on the ϕ_{Eu} of either. For the case of KNCS, the Eu^{3+} phosphorescence of $Eu(btfa)_3$ is unaffected but is quenched for $Eu(hfaa)_3$.

From the CT absorptions of $Eu(NCS)^{2+}$ and $EuBr^{2+}$ species[5], and the singlet levels of hfaa and btfa, (Figure 6.2), it is seen that the CT level due to the added salt lies below the ligand S_{n,π^*} only in the case of $Eu(hfaa)_3$ in the presence of NCS^-.

The transfer, $S_{n,\pi^*} \rightarrow CT$, may occur either intramolecularly in mixed complexes such as $(Eu(aa)_n(NCS)_m)^{3-m-n}$, or intermolecularly.

Europium acetylacetonate does not emit Eu^{3+} phosphorescence in non-polar solvents, indicating that solvent shifts are insufficient to reverse the order of the S_{n,π^*} and CT levels. These shifts are likely to be smaller for coordination compounds than for discrete organic molecules due to the relatively small solvent interaction in the region of the metal-ligand bond.

References

Chapter 6.

1. W.R. Dawson et al., J. Chem. Phys., 45 (1966) 2410.
2. J.S. Brinsen et al., J. Chem. Phys., 42 (1965) 4213; W.F. Sager et al., J. Phys. Chem., 69 (1965) 1092.
3. K. J. Eisentraut et al., J. Amer. Chem. Soc., 87 (1965) 5254.
4. L.J. Nujent et al., J Phys. Chem., 77 (1973) 1528.
5. J.C. Barnes, J. Chem. Soc., (1964) 3880.
6. V.L. Ermolaev et al., Opt. Spectry., 28 (1970) 113.
7. J.P. Fackler Jr. et al., Inorg. Chem., 2 (1963) 97.
8. W.M. Latimer, Oxidation Potentials, 2nd ed., Prentice-Hall, Englewood Cliffs, 1952.
9. M.F. Richardson et al., J. Inorg. Nucl. Chem., 28 (1966) 3005.
10. R.G. Charles et al., J. Inorg. Chem., 28 (1966) 3005.
11. Y Haas et al., J. Phys. Chem., 74 (1970) 2558.

Chapter 7

The Phosphorescence of Group I and Group II Metal Acetylacetonates in Ethanol Glass at 77K

7.1 Introduction

The β-diketoenolate complexes of diamagnetic ions have been shown to phosphoresce at low temperatures in solid matrices[1-4]. This behaviour has been attributed to a radiative transition from the lowest triplet state of the ligand to the ground state and can be quite efficient in the absence of intervening energy levels of the metal ion. Attention has been given largely to dibenzoylmethanato[1,2] and acetylacetonato[3,4] complexes of several diamagnetic metals but with the exception of $Mg(aa)_2$[4] the phosphorescence emission characteristics of the Group I and Group II metal complexes have been neglected. In this chapter are reported the results of investigations of the phosphorescence shown by the diamagnetic acetylacetonate complexes of Li, Na, K, Rb, Cs, Mg, Ca, Sr, and Ba in ethanol glasses at 77K.

7.2 Results and discussion

The absorption spectra of some Group I and Group II metal acetylacetonate complexes in ethanol solution have been discussed by Holm and Cotton[5] and the near symmetric absorption band which occurs in the 280 - 290 nm region assigned as a π, π^* transition of the acetylacetonate ligand. It has been observed that excitation within this absorption band of solid ethanol solutions of the acetylacetonate complexes of Li^+, Na^+, K^+, Rb^+, Cs^+, Mg^{2+},

Ca^{2+}, Sr^{2+} and Ba^{2+} at 77K gives rise to a blue phosphorescence. The emission profiles and the decay characteristics of the phosphorescence shown by these complexes have been measured. The emission profiles obtained with the various complexes were identical, within the limits of experimental error, and consist of a broad band devoid of any pronounced vibrational structure and with maximum emission at ca. 400 nm. The emission profiles are very similar to that given by ethanolic solutions of $Al(aa)_3$ at 77K. In contrast to the similarities in emission profiles, the decay characteristics of the phosphorescence after excitation varied very considerably through the series of complexes. Further, with all the Group I and Group II complexes examined the decay curves showed significant and in some cases very marked deviations from simple exponential behaviour. For example, a very pronounced deviation from simple exponentiality was observed in the case of the caesium complex, whereas the lithium complex showed a much smaller though significant deviation. This may be contrasted with the behaviour of the $Al(aa)_3$ complex where the decay curve was exponential with a measured lifetime, τ = 0.336 s (10^{-2} mol dm^{-3} in ethanol glass at 77K). Previous workers have also found exponential decay for the phosphorescence of $Al(aa)_3$ with reported lifetimes at 77K of τ = 0.362 s in 4:1 ethanol-methanol glass[3], and τ = 0.335 s in EPA[4].

The non-exponential behaviour of the Group I and Group II acetylacetonates suggests that more than one emitting species may be present in the solid solutions. If it is assumed that only two emitting species are present, then the emission intensity at time t after excitation should follow:

$$i(t) = A.\exp(-t/\tau_1) + B.\exp(-t/\tau_2) \qquad \ldots\ldots \quad 7.1$$

where, τ_1 and τ_2 are the exponential lifetimes of the two species, and A and B are coefficients for each first-order process. Making this assumption and that $\tau_2 \ll \tau_1$, the best fit values of τ_1 and τ_2 to the experimental decay data have been computed and a satisfactory fit obtained in all cases. A representative set of results and the computed best fit to a function of type 7.1 is shown in Figure 7.1. The computed values of τ_1 and τ_2 are given in Table 7.1. The validity of the initial assumption that only two emitting species are responsible for the phosphorescence is given considerable support by the values of τ_2 which are constant, within experimental error, at 0.48 $\pm$ 0.04 s which further suggests that one species is common to all solutions. The values of τ_1 do, however, show considerable variations, and decrease monotonically (with the possible exception of the rubidium complex) with increasing cation mass, through each series of acetylacetonates. The ratio τ_2/τ_1 varies from ca. 3 (Li) to 11 (Cs), and it should therefore be possible in principle to obtain the emission spectra of both species by time-resolved spectroscopy. Using the phosphorescence accessory of the spectrofluorimeter, various delays of between 0.05 and 0.5 s were introduced between excitation of the samples and the subsequent detection of the emission. No significant variation of the emission spectra with different delays was observed, indicating that the emission spectra of the two species are identical, within experimental error. It was evident, from consideration of the values of the derived pre-exponential terms and lifetimes, that, in all cases, the major proportion of the phosphorescence was due to the longer lifetime component.

A possible explanation of these results is that the common species in all the glasses is the free acetylacetonate anion with a phosphorescence lifetime τ_2. The lifetime τ_1 may be attributed

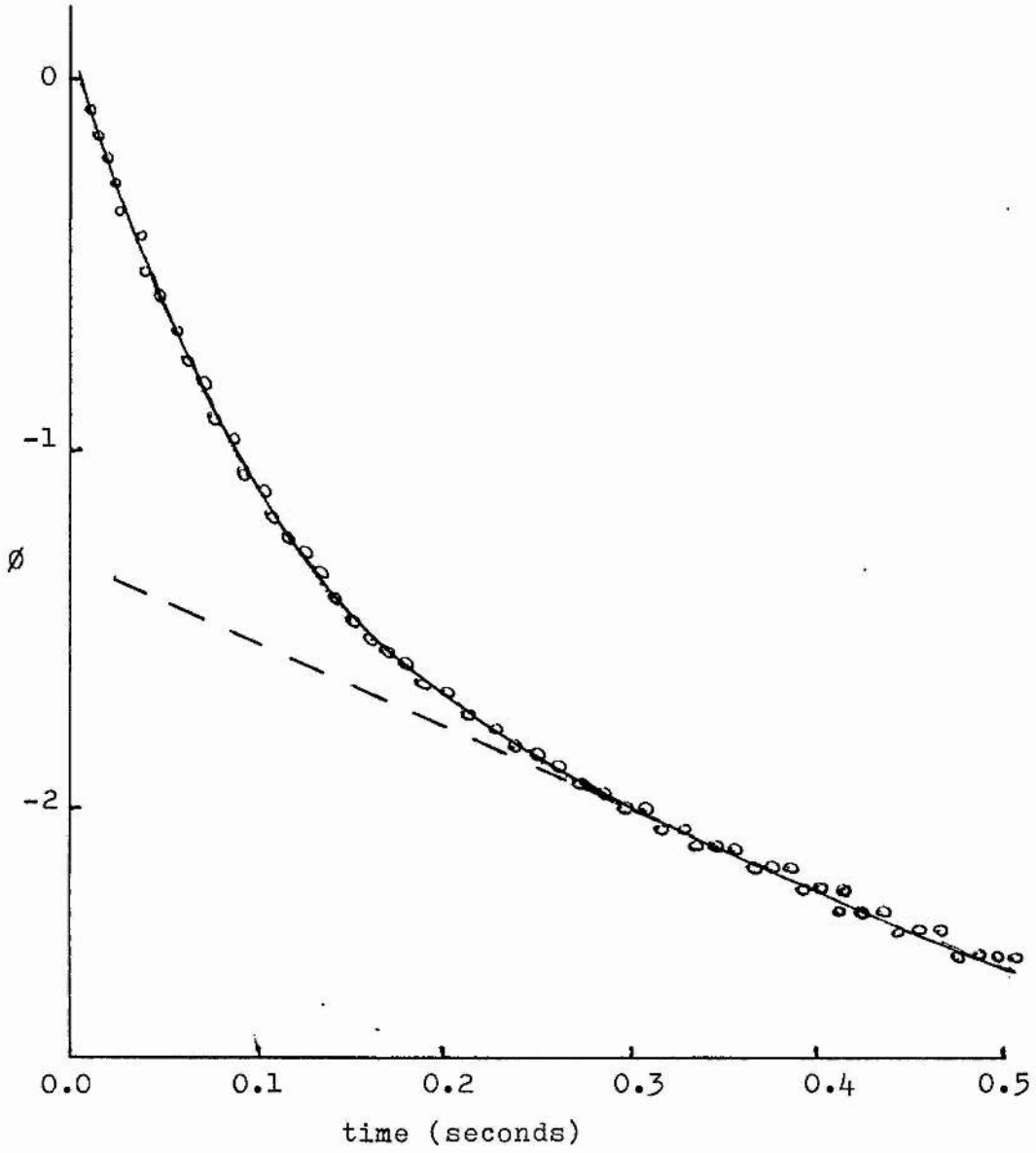

The non-exponential phosphorescence decay of 10^{-2} mol dm^{-3} K(aa) in ethanol at 77 K (o o o o) and the computed best fit (———) to a function (equation 7.1), with τ_1 = 0.058 s and τ_2 = 0.50 s

Figure 7.1

Metal	τ_1 (s) ± 10%	τ_2 (s) ± 0.05
Li	0.151	0.50
Na	0.076	0.46
K	0.058	0.50
Rb	0.063	0.48
Cs	0.045	0.49
Mg[a]	0.183	0.53
Ca	0.130	0.46
Sr	0.069	0.44
Ba	0.063	0.47

a. Clark and Connors[4] have reported a lifetime of 0.325 ± 0.02 s for this compound in EPA at 77 K

Values of τ_1 and τ_2 computed from the emission decays, i(t), of solid ethanol glasses containing 10^{-2} mol dm^{-3} metal acetylacetonate complexes at 77 K

Table 7.1

to the coordinated acetylacetonate ligand in the relevant complexes M(aa), $M'(aa)_2$ and $(M'(aa))^+$, where, M and M' are the Group I and Group II metal ions, respectively. The observed variation in τ_1 can then be associated with changes in the metal ion.

This interpretation requires that appreciable concentrations of free acetylacetonate ion exist in the 10^{-2} mol dm^{-3} glasses. Some information is available regarding the stability constants in ethanol solution at 298K, i.e. log K = 4.6, 2.8, and 2.1 for Li(aa), Na(aa), and K(aa), respectively[6]. The corresponding values of log K for Rb(aa) and Cs(aa) are likely to be < 2.1, the caesium complex being the less stable. Although these values do not give any direct indication of the degree of dissociation of the alkali metal complexes in ethanol glass at 77K, since neither the relevant free energy change nor the rate of attainment of equilibrium during the cooling process is known, they do at least provide upper limits to the likely concentrations of free anion. The calculated dissociations using these figures for a total concentration of 10^{-2} mol dm^{-3} at 293K are 5% (Li), 33% (Na), and 58% (K). For comparison, aluminium acetylacetonate has log K_3 = 5.8[7] in aqueous solution at 303K. Since the corresponding log K_3 in ethanol is likely to be at least one unit higher, less than 0.5% free acetylacetonate anion is expected in 10^{-2} mol dm^{-3} ethanol solution. The relative ordering of these stability constants is therefore in broad agreement with:

a) the substantial deviations from exponential behaviour found with Na(aa) and K(aa);

b) the smaller deviation with Li(aa); and,

c) the absence of any observable deviation with $Al(aa)_3$.

The reported value of log K_2 = 2.54 for $Mg(aa)_2$ in aqueous solution[8] suggests that appreciable dissociation of the Group II complexes in the ethanol glasses is also probable. The possibility that the observed phosphorescence emission could be caused in part by acetylacetone, metal ethoxide or impurities in the ethanol has also been examined. In no case was any observed emission sufficiently intense to make any significant contribution. $Be(aa)_2$ has not been examined, but the high stability of this complex[8,9] relative to the other Group I and Group II metal acetylacetonates suggests that its phosphorescence decay will be near exponential at concentrations of ca. 10^{-2} mol dm^{-3}.

The model proposed above to account for the non-exponential phosphorescence decay requires the values of τ_1 and τ_2 to be independent of the total complex concentration, while the ratio of the pre-exponential terms, A/B, should be concentration dependent in so far as the relative concentrations of coordinated and free acetylacetonate anion.

No significant variations have been detected in the values of A/B, τ_1, or τ_2 obtained over the rather restricted range of concentration which is experimentally accessible with our present equipment i.e. ca. 10^{-2} - 5 x 10^{-2} mol dm^{-3}. We have also found that the presence of added metal hydroxide at concentrations up to five times that of the metal acetylacetonate does not alter the profile of the decay curve.

The stability constants for the Group I acetylacetonates imply that near complete dissociation should occur in ethanolic solutions of ca. 10^{-4} mol dm^{-3}, i.e. the concentration region in which absorption spectra are readily measured. However the λ_{max} values reported by Holm and Cotton[5] for ethanol solutions ($< 10^{-4}$ mol dm^{-3})

of the Group I (and Group II) acetylacetonates vary quite markedly with change in the metal ion contrary to the constant profile of the free acetylacetonate anion expected from the stability data above. The absorption spectra of these complexes have been determined in ethanol solution over the concentration range 10^{-3} - 10^{-5} mol dm^{-3}. It was found that the absorption profiles were critically dependent on the concentration and the temperature, and also varied with time. Two distinct spectral profiles were observed:

a) as the concentration approached 10^{-3} mol dm^{-3}, the profile tended towards a near symmetrical absorption band with λ_{max} = 293 ± 2 nm for the Group I and Group II complexes; and,

b) as the concentration decreased towards 10^{-5} mol dm^{-3}, the λ_{max} was blue shifted to give ultimately an absorption band identical to that of acetlacetone in ethanol with λ_{max} = 274 nm. This behaviour can be rationalised in terms of solvolysis of the acetylacetonate anion leading to the production of free acetylacetone. Similar behaviour has been observed in ethanol solutions of the lanthanoid complexes, $Ln(aa)_3.3H_2O$ and with $Th(aa)_4$. The absorption band at ca. 293 nm observed in the more concentrated solutions of all the complexes, with the exception of $Mg(aa)_2$ (λ_{max} = 285 nm at 5.6 x 10^{-3} mol dm^{-3}), may be attributed largely to absorption of the free acetylacetonate anion. There will probably however be significant amounts of coordinated ligand also present at concentrations close to 10^{-3} mol dm^{-3}, and the small variation in λ_{max} indicates that coordination to these ions has relatively little effect on the π,π^* singlet absorption of the acetylacetonate ligand. This supports the previous suggestion that the phosphorescence spectra of coordinated and free acetylacetonate anion are very siminar. In aqueous solutions of Li(aa), Na(aa), and K(aa),

no hydrolysis effects were observed and a constant absorption profile with λ_{max} = 292 nm was found, in agreement with previous results[5]. This absorption may be attributed entirely to the acetylacetonate anion.

It is apparent from these investigations that the triplet state lifetime is a much more sensitive diagnostic for investigating the environment of the acetylacetonate anion than either absorption or emission spectroscopy.

References

Chapter 7.

1. P. Yuster et al., J. Chem. Phys., 17 (1949) 1182.
2. H. Levanon, Chem. Phys. Lett., 9 (1971) 257.
3. G.A. Crosby et al., J. Chem. Phys., 55 (1971) 4663.
4. R.H. Clarke et al., Spect. Acta, 30A (1974) 2063.
5. R.H. Holm et al., J. Amer. Chem. Soc., 80 (1958) 5658.
6. D.C. Luehrs et al., Inorg. Chem., 4 (1965) 1739.
7. R.M. Izatt et al., J. Phys. Chem., 59 (1955) 170.
8. R.M. Izatt et al., J. Phys. Chem., 59 (1955) 80.
9. R.W. Green et al., J. Phys. Chem., 67 (1963) 905.

Chapter 8

EPILOGUE

Intermolecular energy transfer occurs between $Tb(aa)_3.3H_2O$ and $Ln(aa)_3.3H_2O$ complexes (Ln = Pr, Nd, Sm, Eu, Dy, Ho or Er; aa = acetylacetonate) in n-butanol solution at 293K.

Measurement of the decay time of the Tb^{3+} $^5D_4$ level indicates that transfer occurs from this level to excited levels of the Ln^{3+} ions with bimolecular rate constants within the range 0.5 - 4.9 x 10^5 dm^3 mol s^{-1}.

Data from similar measurements on a mixed crystal $Eu_xTb_{(1-x)}(aa)_3.3H_2O$ and other considerations indicate that this is a very short range electron-exchange transfer.

Similar measurements of the Tb^{3+} ion phosphorescence yield indicate the presence of a further intermolecular transfer process between a higher excited state of the Tb^{3+} complex and the added Ln^{3+} complexes. The Stern-Volmer quenching constants vary from 11 dm^3 mol^{-1} for Ho and Sm to 110 dm^3 mol^{-1} for Pr. It is concluded that this transfer is unlikely to occur from either the ligand singlet or triplet levels and it is proposed that a higher Tb^{3+} level such as the $^5D_3$ may be involved in both inter- and intramolecular energy transfer.

Some future work could be to attempt the measurement of the $^5D_3$ lifetime and, if the quantum yield is high enough, to attempt a study of Ln^{3+} quenching of this level in an analogous manner to that on the $^5D_4$ level.

Intermolecular energy transfer betwwen excited state Tb^{3+} ions in $Tb(aa)_3.3H_2O$ and Ln^{3+} ions in $Ln(aa)_3.3H_2O$, where Ln = Eu and Sm, is shown to be markedly solvent dependent. It is proposed that the $Tb^{3+} \rightarrow Ln^{3+}$ energy transfer occurs in mixed metal dimers where the Tb-Ln distance is likely to be ca. 0.4 nm.

The solvent dependent behaviour is related to the relative concentrations of monomeric and dimeric species in the various solvents. The rate controlling step in the intermolecular energy transfer is probably that of monomer-dimer reaction which at 273K is of the order of 10^5 dm^3 mol^{-1} s^{-1}. The activation energy of this reaction between Tb, Eu and Sm acetylacetonates is estimated to be ca. 23 kJ mol^{-1}.

The nature of the proposed monomer-dimer interaction could be assessed more precisely by a careful study of the mixing experiment using more suitable apparatus.

^1H NMR spectra of $Lu(aa)_3.2H_2O$ in several solvents are reported.

The spectral profiles are temperature dependent in benzene and toluene solutions and the multiplicity of ligand methyl resonances is attributed to slow exchange between non-equivalent methyl groups in a dimeric structure.

The temperature dependence in acetone solution is consistent with the presence of a monomer-dimer equilibrium with $\Delta H^o = -28.2 \pm 1.5$ kJ mol^{-1} and $\Delta S^o = -74.5 \pm 4.5$ J K^{-1} mol^{-1}.

The single ligand methyl and 3-H resonances in the

strongly coordinating solvents dimethyl sulphoxide and pyridine indicate the sole presence of solvated monomers.

Previous proposals about the anomalous spectrum of $Mg(aa)_2$ in $CDCl_3$ are also discussed.

The extremely low efficiency of the intermolecular energy transfer process in europium acetylacetonate compared with the corresponding terbium acetylacetonate is attributed to the presence of a charge-transfer excited state lying below the ligand singlet states. This is supported by the anomalous absorption spectrum of the Eu^{3+} complex and the effects of added anions in other ligand systems.

The phosphorescence spectra of the Group I and Group II metal acetylacetonates (Metal = Li, Na, K, Rb, Cs, Mg, Ca, Sr and Ba) have all been measured in solid ethanol glass solutions at 77K and found to have profiles similar to that of $Al(aa)_3$.

The phosphorescence decays are non-exponential and this behaviour is attributed to the presence of both coordinated and free acetylacetonate anion.

Time resolved spectroscopy and other considerations indicate that the energies of the lowest excited ligand singlet and triplet states of the aa^- ion are, unlike the triplet state lifetime, little affected by coordination.

Solvolysis is reported in ethanol solution which invalidates some previously reported spectral parameters.